iScience

CellPress
OPEN ACCESS

Article

Dickkopf-2 regulates the stem cell marker LGR5 in colorectal cancer via HNF4α1

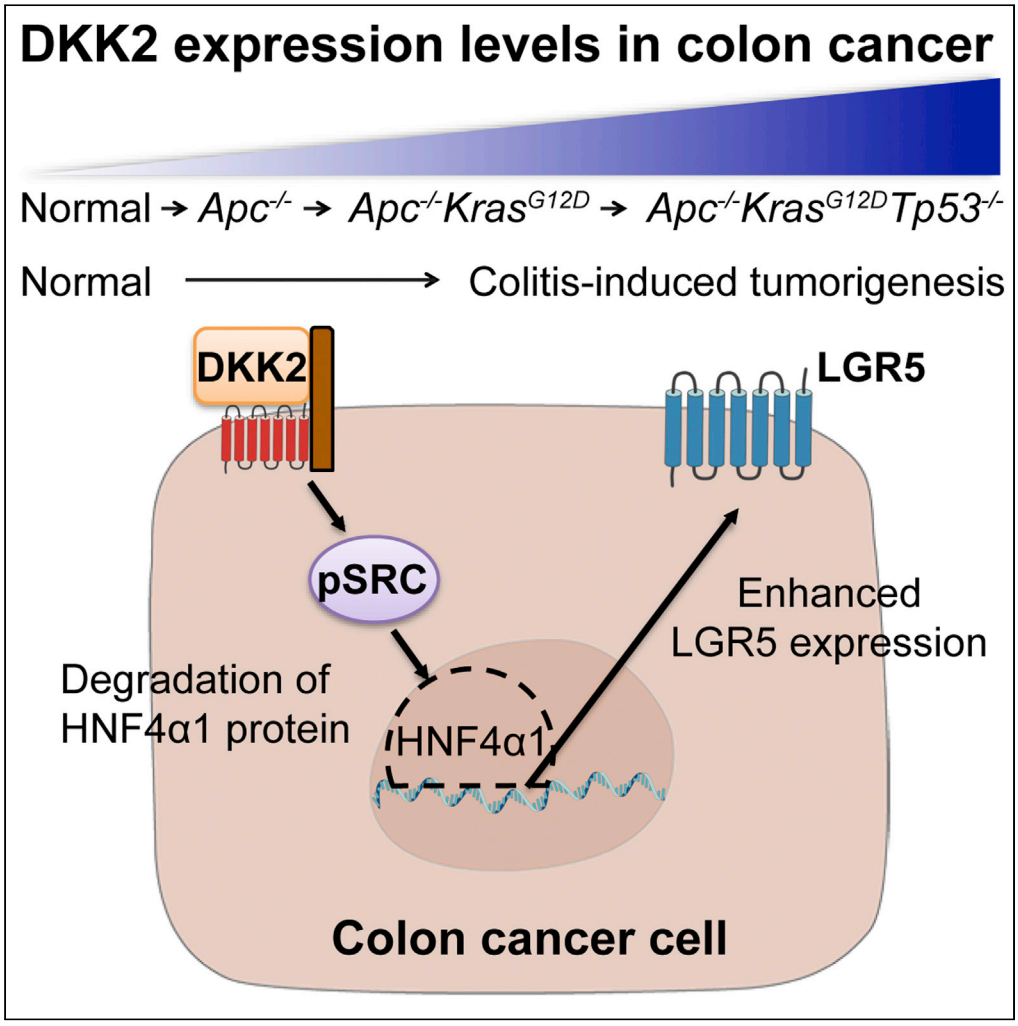

Jae Hun Shin, Jaekwang Jeong, Jungmin Choi, ..., Omer Yilmaz, Je-Min Choi, Alfred L.M. Bothwell

alfred.bothwell@yale.edu

Highlights

APC, *KRAS*, and *TP53* mutations induce DKK2 expression in murine colon cancer

DKK2 increases Src phosphorylation in colon cancer cells

Activated Src leads to degradation of HNF4α1 protein

This DKK2 downstream signaling enhances LGR5 expression in colon cancer

Shin et al., iScience *24*, 102411
May 21, 2021 © 2021 The Authors.
https://doi.org/10.1016/j.isci.2021.102411

iScience

CellPress
OPEN ACCESS

Article

Dickkopf-2 regulates the stem cell marker LGR5 in colorectal cancer via HNF4α1

Jae Hun Shin,[1] Jaekwang Jeong,[2] Jungmin Choi,[3,4] Jaechul Lim,[1] Ravi K. Dinesh,[1] Jonathan Braverman,[5] Jun Young Hong,[1] Stephen E. Maher,[1] Maria C. Amezcua Vesely,[1] WonJu Kim,[7] Ja-Hyun Koo,[7] Wenwen Tang,[8] Dianqing Wu,[8] Holly N. Blackburn,[1,9] Rosa M. Xicola,[10] Xavier Llor,[10] Omer Yilmaz,[5,6] Je-Min Choi,[7] and Alfred L.M. Bothwell[1,11,*]

SUMMARY

Enhanced stemness in colorectal cancer has been reported and it contributes to aggressive progression, but the underlying mechanisms remain unclear. Here we report a Wnt ligand, Dickkopf-2 (DKK2) is essential for developing colorectal cancer stemness. Genetic depletion of *DKK2* in intestinal epithelial or stem cells reduced tumorigenesis and expression of the stem cell marker genes including *LGR5* in a model of colitis-associated cancer. Sequential mutations in *APC, KRAS, TP53,* and *SMAD4* genes in colonic organoids revealed a significant increase of *DKK2* expression by APC knockout and further increased by additional *KRAS* and *TP53* mutations. Moreover, DKK2 activates proto-oncogene tyrosine-protein kinse Src followed by increased LGR5 expressing cells in colorectal cancer through degradation of HNF4α1 protein. These findings suggest that DKK2 is required for colonic epithelial cells to enhance LGR5 expression during the progression of colorectal cancer.

INTRODUCTION

Colorectal cancer is the third most common cancer in the world and the second leading cause of cancer related death (Bray et al., 2018). About 80% of colorectal cancer patients have mutations in the adenomatous polyposis coli (*APC*) gene, a negative regulator of canonical Wnt signaling (Phelps et al., 2009). *APC* mutations in stem cells initiate intestinal tumorigenesis (Barker et al., 2009). Barker et al. has identified *LGR5* as an intestinal stem cell marker gene (Barker et al., 2007). LGR5 positive intestinal stem cell-specific *APC* conditional knockout mice showed spontaneous tumor formation whereas *APC* deletion in non-stem cells was rarely tumorigenic (Barker et al., 2009). Lineage tracing studies further confirmed LGR5 positive stem cells as cancer stem cells in the gut (Schepers et al., 2012). Additional oncogenic mutations in *KRAS*, *TP53* and *SMAD4* in epithelial cells promote colorectal carcinogenesis (Vogelstein et al., 1988). Briefly, oncogenic alterations in intestinal stem cells lead to initiation and progression of colorectal cancer.

Recent advances in organoid culture techniques allowed *in vitro* primary intestinal epithelial cell culture (Sato et al., 2009; Drost and Clevers, 2018). Mutations in *APC, KRAS, TP53* and *SMAD4* in human intestinal organoids using CRISPR methods provided a better understanding of carcinogenesis in colorectal cancer (Matano et al., 2015). Depletion of LGR5 expressing cancer stem cells in murine primary or metastatic colon cancer cells carrying those mutations have shown the necessity of cancer stem cells in metastatic progression (de Sousa e Melo et al., 2017). However, underlying mechanisms of how LGR5 expressing cancer stem cells arise and are maintained are still elusive.

In this study, we introduce DKK2 as an essential factor for LGR5 expression in colon cancer. We showed increased DKK2 expression in colon tumor epithelial cells. Using colon cancer organoids, we showed a significant increase of *DKK2* transcription by triple mutations in *APC*, *KRAS*, and *TP53* genes. Gain and loss of function studies using normal or cancer organoids revealed a feedforward feedback regulation of DKK2 expression. Mechanistically, we have identified that DKK2 activates proto-oncogene tyrosine-protein kinse Src (c-Src), which then results in HNF4α1 protein degradation followed by enhanced LGR5 expression in colon cancer. Our findings provide a better understanding of the formation of LGR5 expressing cancer stem cells during colorectal cancer progression.

[1]Department of Immunobiology, Yale University School of Medicine, TAC 641D, PO Box 208011, 300 Cedar Street, New Haven, CT 06520-8011, USA

[2]Internal Medicine, Yale University School of Medicine, New Haven, CT 06520, USA

[3]Department of Genetics, Yale University School of Medicine, New Haven, CT 06520, USA

[4]Department of Biomedical Sciences, Korea University College of Medicine, Seoul 02841, Korea

[5]The David H. Koch Institute for Integrative Cancer Research at MIT, Department of Biology, Massachusetts Institute of Technology, Cambridge, MA, USA

[6]Department of Pathology, Massachusetts General Hospital, Boston, MA, USA

[7]Department of Life Science, College of Natural Science, Hanyang University, Seoul 04763, Republic of Korea

[8]Vascular Biology and Therapeutic Program and Department of Pharmacology, Yale University School of Medicine, New Haven, CT 06520, USA

[9]Department of Surgery, Yale University School of Medicine, New Haven, CT 06520, USA

[10]Department of Medicine and Cancer Center, Yale University, New Haven, CT 06520, USA

[11]Lead contact

*Correspondence: alfred.bothwell@yale.edu

https://doi.org/10.1016/j.isci.2021.102411

This is an open access article under the CC BY-NC-ND license (http://creativecommons.org/licenses/by-nc-nd/4.0/).

RESULTS

DKK2 is highly expressed in colorectal cancer epithelium and facilitates tumorigenesis

DKK2 expression is increased about 50-fold in colorectal cancer patients compared to healthy normal controls and polyp-specific DKK2 expression in *APC* mutant ($Apc^{min/+}$) mice has been reported by *in situ* hybridization (Matsui et al., 2009; Gregorieff et al., 2005). We have confirmed the elevation of DKK2 in colorectal cancer using colorectal cancer patient samples and a murine colitis-induced tumor model. Transcriptional increase of *DKK2* was observed in human colorectal carcinoma RNA sequencing (RNA-seq) data along with increased expression of the stem cell marker gene, *LGR5* (Figure 1A). DKK2 expression was increased about 100-fold in tumor tissues compared to untreated controls in the azoxymethane and dextran sodium sulfate (AOM/DSS)-treated colitis-induced tumor model (Figures 1B and 1C). Polyp-specific increase of *DKK2* expression was observed in a time course experiment (Figure 1D). Immunohistochemistry analysis for DKK2 showed epithelial expression of DKK2 in murine colitis-induced tumors (Figure 1E). To confirm the pattern of DKK2 expression, we sorted epithelial cells from colitis-induced tumors based on epithelial marker gene (EpCAM) and stem cell marker gene expression (LGR5) using $Lgr5^{CreERT2\text{-}IRES\text{-}EGFP}$ reporter mice (Figures S1A and S1B). The sorted $LGR5^{high}$, $LGR5^{mid}$, and $LGR5^{neg}$ populations represent intestinal stem cell populations, transit amplifying cell and Paneth cell populations and differentiated epithelial cell populations, respectively (Sato et al., 2009). Increased expression of *DKK2* was shown along with LGR5 expression (Figure 1F). These data demonstrate a significant increase of *DKK2* expression and its pattern in colonic epithelium in the colitis-induced tumor model.

Next, in order to investigate the roles of DKK2 in intestinal tumorigenesis, we generated intestinal epithelium-specific *DKK2* conditional knockout $Villin^{Cre}$-$Dkk2^{fl/fl}$ mice. Eighty days after AOM/DSS treatment, the number and size of polyps were recorded by colonoscopy. DKK2 knockout in the intestinal epithelium showed about 60% reduction of tumor growth (Figures 1G–1J and S1C). Interestingly, *DKK2* knockout does not alter proliferation of colitis-induced tumor cells (Figures S1D and S1E). Rather, the expression of stem cell marker gene *LGR5* was reduced in the absence of DKK2 and there was a correlation of expression between *DKK2* and *LGR5* during colitis-induced tumor development (Figures 1K and 1L). These findings suggest that DKK2 contributes to intestinal tumorigenesis and the elevation of *LGR5* expression in colorectal cancer.

DKK2 depletion modulates stemness and differentiation of colitis-induced tumor cells

Using tamoxifen-inducible intestinal stem cell-specific *DKK2* knockout ($Lgr5^{CreERT2\text{-}IRES\text{-}EGFP}$-$Dkk2^{fl/fl}$) mice, we have confirmed that *DKK2* expression in *LGR5* positive cells and its daughter cells promotes colitis-induced tumorigenesis (Figures 2A–2E). The correlation between *DKK2* and *LGR5* expression was confirmed as well and those results were not a consequence of the functional loss of one *LGR5* promoter allele in the $Lgr5^{CreERT2\text{-}IRES\text{-}EGFP}$-$Dkk2^{fl/fl}$ mice (Figures S1F and S1G).

As an unbiased way to assess the roles of DKK2 in intestinal tumorigenesis, we performed a bulk RNA-seq analysis on colitis-induced polyps from the AOM/DSS-treated $Lgr5^{CreERT2\text{-}IRES\text{-}EGFP}$-$Dkk2^{fl/fl}$ mice. Consistent with the previous $Villin^{Cre}$-$Dkk2^{fl/fl}$ mice data, the expression of LGR5 was decreased in the absence of DKK2 (Figure 2F). Quiescent stem cell marker genes, *BMI1* and *TERT*, were reduced as well whereas the differentiation marker genes, *EMP1*, *KRT20* and *SLC26A3* were increased and it has been confirmed with quantitative PCR analysis (Figure 2G). Again, expression of proliferation marker genes such as *KI67* was unaltered in *DKK2*-deficient polyps (Figure 2G). These results imply that DKK2 regulates stemness and differentiation of epithelial cells in a colitis-induced tumor model.

DKK2 enhances Lgr5 expression in colonic epithelial cells

In the canonical Wnt signaling pathway, DKK2 has been introduced as a Wnt antagonist, binding to the common Wnt receptors, LRP5 and LRP6 (Niehrs, 2006). The following studies have reported the agonistic roles of DKK2 in the canonical Wnt pathway in the absence of another Wnt receptor Kremen2 (Mao and Niehrs, 2003). To test the direct effects of DKK2 on colonic epithelial cells, we performed normal colonic organoid culture in the presence of mouse recombinant DKK2 protein. Notably, expression of the canonical Wnt target genes was unchanged in the cultured organoids after recombinant DKK2 treatment (Figure 3A). Meanwhile, *LGR5* expression was increased about 3-fold compared to the untreated controls (Figure 3B). In addition, recombinant DKK2 treatment further increased *DKK2* expression in organoids in a dose- and time-dependent manner indicating the feedforward regulation of its expression (Figures 3C and 3D).

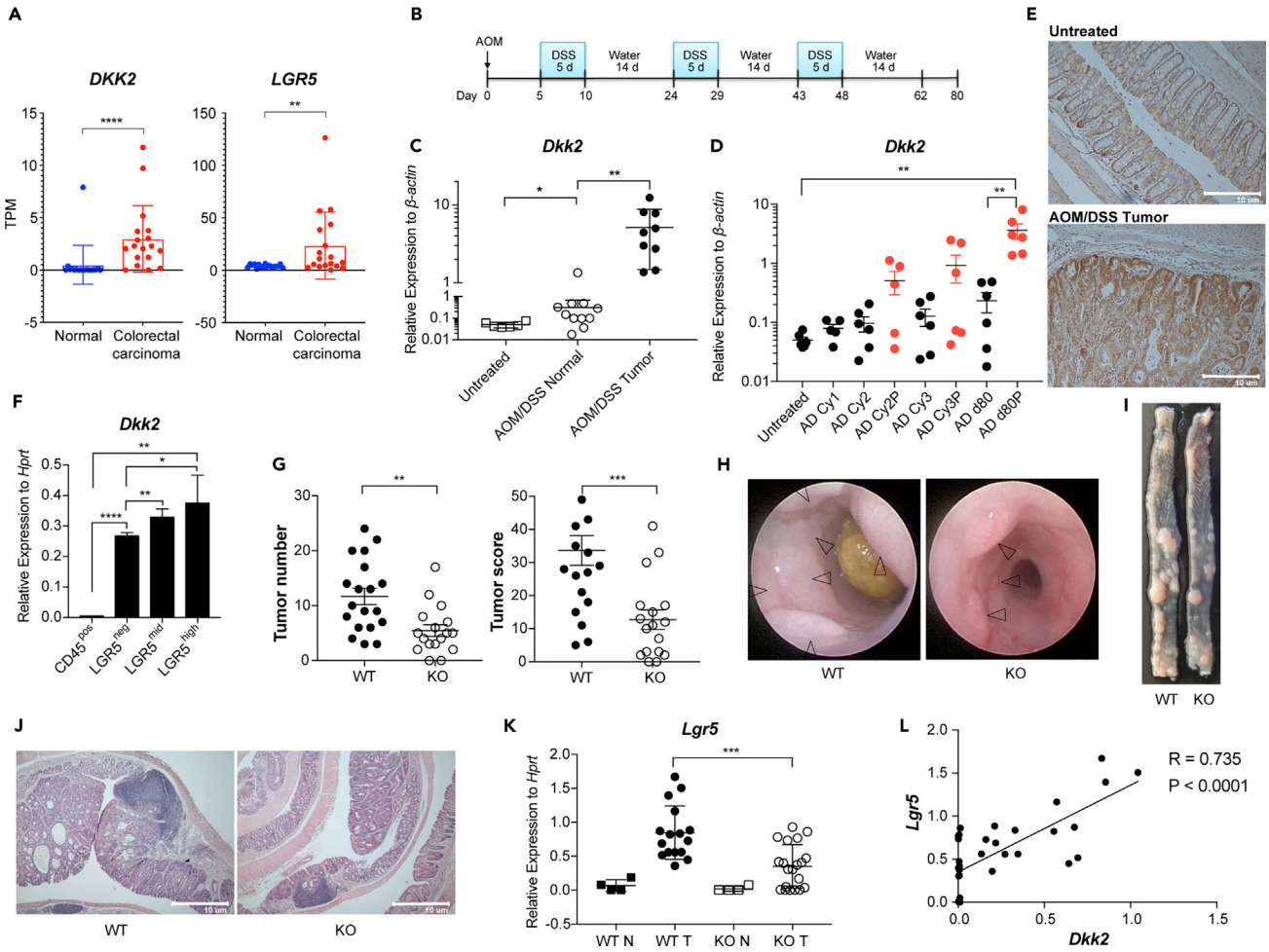

Figure 1. DKK2 expression in colon cancers and reduced colitis-induced tumorigenesis in DKK2 deficient mice

(A) Expression of DKK2 and LGR5 in human colorectal carcinoma and adjacent normal tissues was analyzed using previously deposited RNA-seq data (GSE50760, *n* = 18 each group, TPM; Transcripts per million).

(B) A schematic diagram of azoxymethane/dextran sodium sulfate (AOM/DSS) treatment schedule.

(C) Quantitative PCR analysis of DKK2 expression in mouse colon tissues or polyps upon AOM/DSS treatment. Each symbol indicates an individual tissue sample.

(D) Expression kinetics of DKK2 in the AOM/DSS-treated wild type C57BL/6 colon tissues measured by quantitative PCR (AD; AOM/DSS, Cy1, 2 and 3; the first, second and third DSS cycle, P; polyps, d80; day 80, Red; polyps, Black; normal tissues). Each dot represents an individual tissue sample.

(E) Representative DKK2 immunohistochemistry in AOM/DSS-induced tumors. Scale bar = 10 μm.

(F) Quantitative analysis of DKK2 expression in the sorted tumor cells based on EGFP signal from AOM/DSS treated *Lgr5-EGFP* reporter mice.

(G) Tumor number and score by colonoscopy in wild type (WT, *n* = 19) or *Villin*^{Cre}-*Dkk2*$^{fl/fl}$ knockout (KO, *n* = 17) mice on day 80. *n* represents the number of independent mice.

(H–J) Representative of colonoscopy, macroscopic view and histology on day 80.

(K) Quantitative gene expression analysis of LGR5 in tumor tissues after AOM/DSS treatment. WT N: wild type normal colon, *n* = 4, WT T: wild type tumor, *n* = 16, KO N: *Dkk2* knockout normal colon, *n* = 4, KO T: Dkk2 knockout tumor, *n* = 20. *n* represents the number of tumor tissues.

(L) Correlation of DKK2 and LGR5 relative expression to *Hprt* in tumor samples by Pearson r test. Each dot represents an individual tissue sample. n.s, not significant, *p < 0.05, **p < 0.01, ***p < 0.001, ****p < 0.0001; two-tailed Welch's ttest. Error bars indicate mean ± s.d. Results are representative of three independent experiments.

Next, we questioned whether our *in vitro* findings are reproducible in tumor settings. In order to understand the expression conditions of DKK2 during colorectal cancer development, we generated colon cancer organoids carrying various combinations of mutations in *APC*, *KRAS*, *TP53*, and *SMAD4* genes that are commonly observed during colorectal cancer progression (Vogelstein et al., 2013) (Figure 3E). Accumulating mutations in those genes resulted in the elevation of LGR5 expression in colonic organoids (Figure S2A). Expression of *DKK2* was detected in *Apc knockout* (A) and *Apc knockout Kras*^{G12D} (AK) mutant organoids (Figure 3F). It was further increased in *Apc*

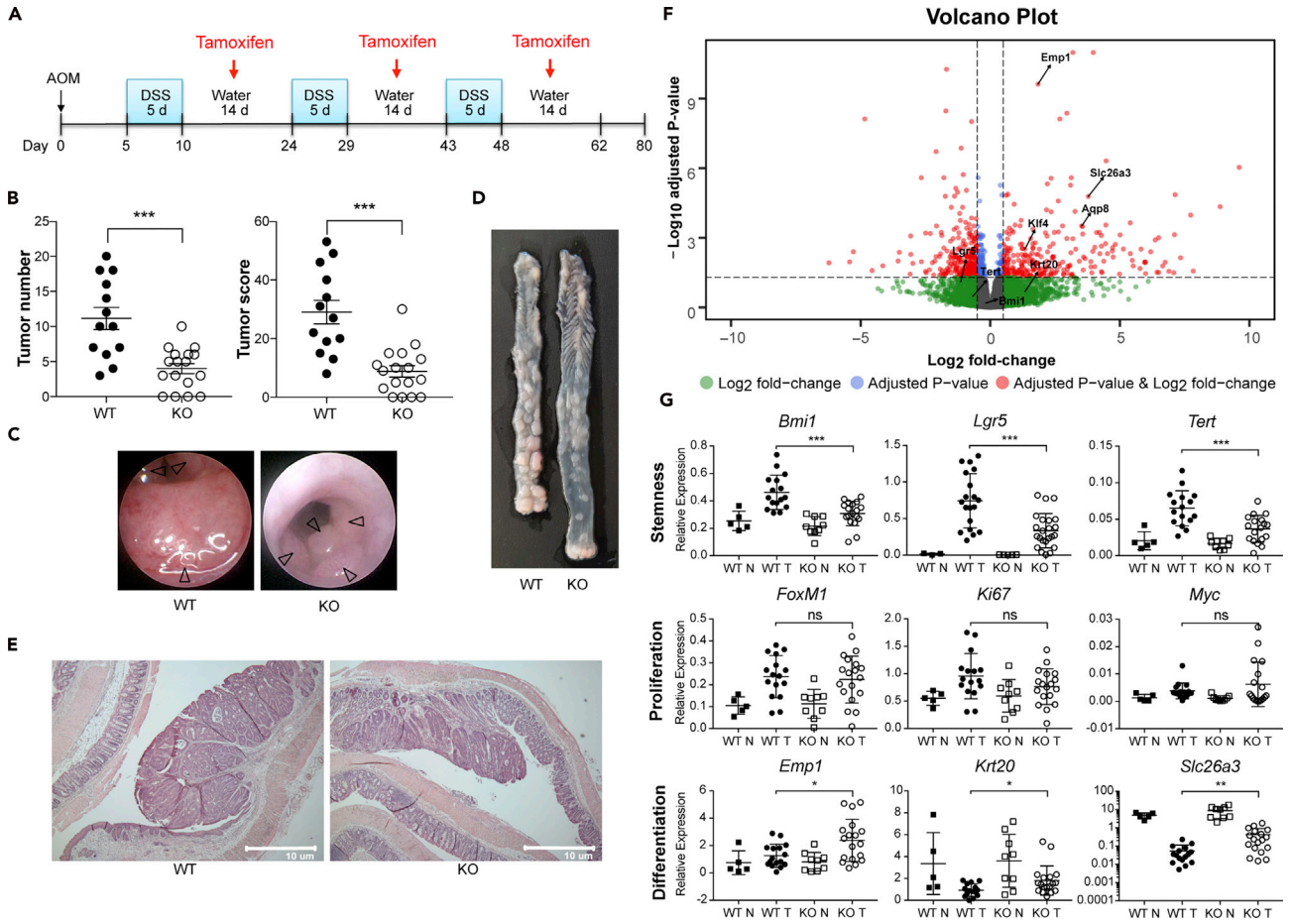

Figure 2. DKK2 regulates stemness and differentiation of colon cancer cells

(A) A schematic diagram of AOM/DSS treatment schedule with tamoxifen administration in order to knockout DKK2 in LGR5 positive cells. 2 mg of tamoxifen was administered by intra-peritoneal injection every other day from day 7 after DSS water was removed.

(B) Tumor number and score by colonoscopy in wild type (WT, n = 13) or $Lgr5^{CreERT2}$-$Dkk2^{fl/fl}$ knockout (KO, n = 17) mice on day 80.

(C–E) Representative view of colonoscopy, macroscopic view and histology at the same time.

(F) Volcano plot generated by RNA-seq analysis for AOM/DSS-induced tumors from wild type and $Lgr5^{CreERT2}$-$Dkk2^{fl/fl}$ knockout mice. Wald test, *Lgr5*; p = 0.004, adjust p = 0.078, *Tert*; p = 0.070, adjust p = 0.336, *Bmi1*; p = 0.290, adjust p = 0.639, *Aqp8*; p = 1.07 × 10^{-6}, adjust p = 0.003, *Emp1*; p = 6.01 × 10^{-14}, adjust p = 2.39E-10, *Krt20*; p = 0.025, adjust p = 0.206, *Klf4*; p = 2.99 × 10^{-5}, adjust p = 0.003, *Slc26a3*; p = 3.32 × 10^{-8}, adjust p = 1.65 × 10^{-5}.

(G) Quantitative gene expression analysis of AOM/DSS-induced tumors in stem cell maker genes (*Bmi1*, *Lgr5* and *Tert*), proliferation marker genes (*FoxM1*, *Ki67* and *Myc*) and differentiation marker genes (*Emp1*, *Krt20* and *Slc26a3*). WT N: wild type normal colon, WT T: wild type tumor, KO N: *Dkk2* knockout normal colon, KO T: *Dkk2* knockout tumor. Each *symbol* represents an individual tissue sample. n.s, not significant, *p < 0.05, **p < 0.01, ***p < 0.001; two-tailed Welch's ttest. Error bars indicate mean ± s.d.

knockout $Kras^{G12D}$ and *Tp53 knockout* triple mutant (AKP) organoids and this expression level was maintained in quadruple mutant (AKPS) organoids with additional knockout in the *SMAD4* gene (Figure 3F). Given that information, AKP organoids were used for the following experiments.

The time course expression of *DKK2* and *LGR5* in AKP organoids was analyzed for 10 days after single isolated cells were embedded in 3-dimensional matrigel culture. *DKK2* expression increased and reached a plateau at day 8 (Figure S2B). *LGR5* expression increased at day 4-6 when spheroids formed then decreased about two-fold and was maintained at day 8-10 when enteroid formation was mostly observed (Figure S2C). Based on these results, we decided to perform transcriptome analysis at day 8.

We then developed DKK2 knockout AKP (KO) organoids using the CRISPR technique. To rule out unwanted results by Cas9-driven random mutations on *DKK2*, we cloned *DKK2* knockout AKP organoids through single cell sorting and sequencing (Figure S2D). The identified clones could only express truncated DKK2 protein

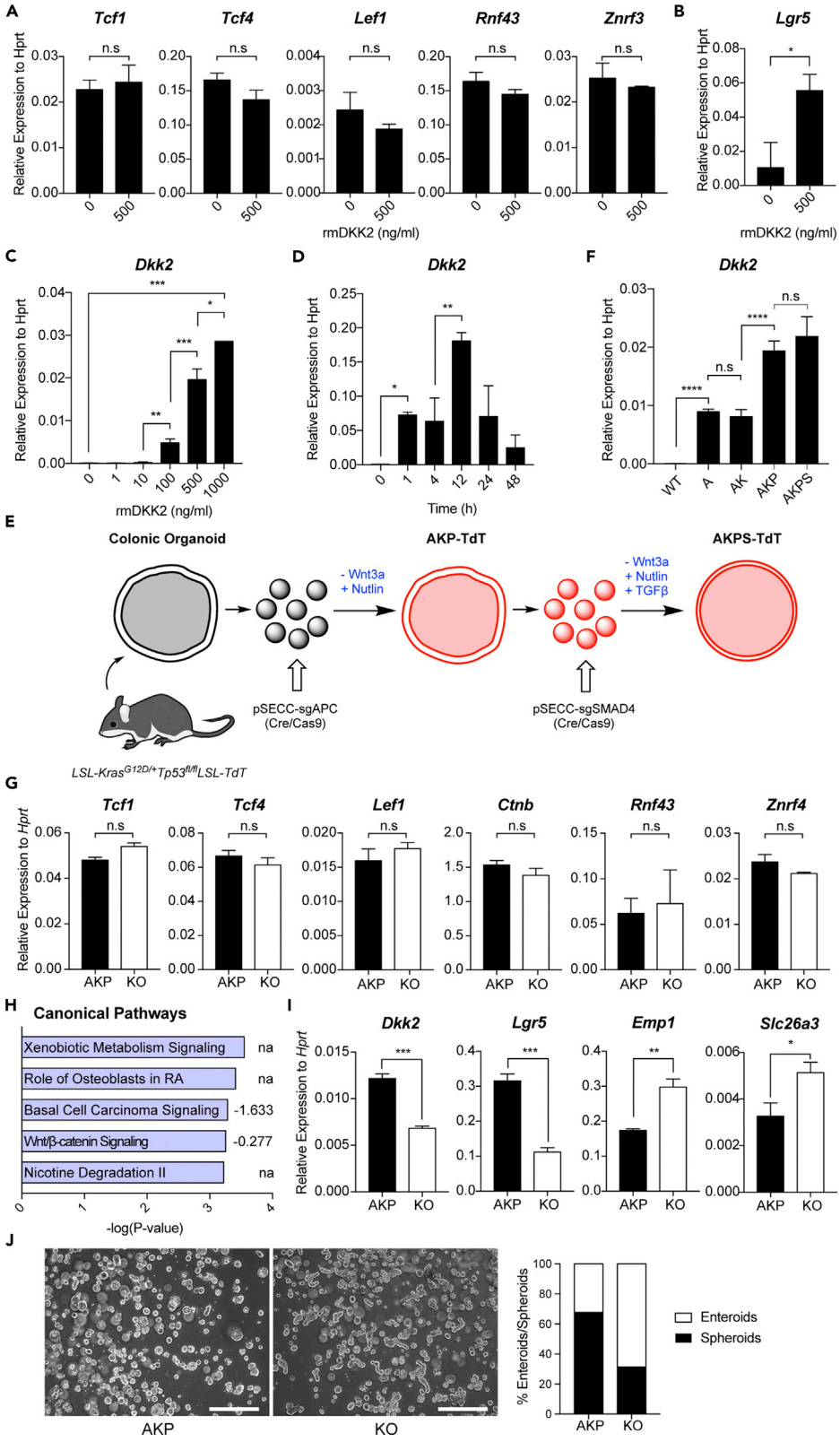
A
Tcf1
Tcf4
Lef1
Rnf43
Znrf3
Relative Expression to Hprt
n.s
rmDKK2 (ng/ml)
B
Lgr5
*
C
Dkk2
rmDKK2 (ng/ml)
D
Dkk2
Time (h)
F
Dkk2
WT
A
AK
AKP
AKPS
E
Colonic Organoid
AKP-TdT
AKPS-TdT
- Wnt3a
+ Nutlin
- Wnt3a
+ Nutlin
+ TGFβ
pSECC-sgAPC
(Cre/Cas9)
pSECC-sgSMAD4
(Cre/Cas9)
LSL-KrasG12D/+Tp53fl/flLSL-TdT
G
Tcf1
Tcf4
Lef1
Ctnb
Rnf43
Znrf4
Relative Expression to Hprt
AKP
KO
H
Canonical Pathways
Xenobiotic Metabolism Signaling
na
Role of Osteoblasts in RA
na
Basal Cell Carcinoma Signaling
-1.633
Wnt/β-catenin Signaling
-0.277
Nicotine Degradation II
na
-log(P-value)
I
Dkk2
Lgr5
Emp1
Slc26a3
Relative Expression to Hprt
J
AKP
KO
% Enteroids/Spheroids
Enteroids
Spheroids

Figure 3. DKK2 enhances *Lgr5* expression in intestinal epithelial cells without affecting expression of the canonical Wnt target genes

Normal colonic organoids were cultured in the presence or absence of recombinant DKK2 for 3 days (rmDKK2: Recombinant mouse DKK2 protein).

(A and B) Quantitative gene expression analyses of the canonical Wnt target genes (A) and Lgr5 (B).

(C and D) *Dkk2* expression after rmDKK2 treatment in a dose- (C) and time-dependent (D) manner.

(E) A schematic diagram of colon cancer organoid development. *Apc, Kras* and *Tp53* triple (AKP) and plus *Smad4* quadruple (AKPS) organoids are shown. Colonic organoids were generated from *LSL-Kras*$^{G12D/+}$*Tp53*$^{fl/fl}$*LSL-TdT* mice. AKP triple mutations were acquired by adenoviral transduction of pSECC plasmids carrying Cre, Cas9 and guide RNA targeting *Apc* to isolated single organoid cells. Mutant tumor organoids were selected during culture in the absence of Wnt3a, EGF and Nutlin recombinant proteins for *Apc, Kras* and *Tp53* mutations, respectively. Additional adenoviral transduction and recombinant TGFβ selection were performed to incorporate *Smad4* mutations in order to generate AKPS organoids. *LSL: LoxP-Stop-Loxp, TdT*: Tandem dimer Tomato.

(F) *Dkk2* expression in wild type (WT) colonic organoids and colon cancer organoids carrying Apc mutation (A), *Apc* and *Kras* mutations (AK), *Apc, Kras* and *Tp53* mutations (AKP) and *Apc, Kras, Tp53* and *Smad4* mutations (AKPS).

(G) Expression of the canonical Wnt target genes in *Dkk2* knockout AKP (KO) organoids.

(H) Ingenuity pathway analysis of colitis-induced tumor RNA-seq data suggested canonical pathways by *Dkk2* knockout. Numbers indicate activation *Z* score.

(I) Expression of *Dkk2, Lgr5, Emp1* and *Slc26a3* in KO organoids.

(J) Representative pictures and the percentiles of spheroid versus enteroids in control and KO organoids. Cystic organoids were counted as spheroids while budding shape organoids were counted as enteroids. 20 independent images were analyzed in each group. Scale bar = 50 μm. n.s, not significant, *p < 0.05, **p < 0.01, ***p < 0.001, ****p < 0.001; two-tailed Welch's ttest. Error bars indicate mean ± s.d.

(Figure S2E). While the CRISPR technique does not alter target gene transcription, we observed more than 50% reduction in DKK2 expression after knockout, indicating that the positive feedback regulation in DKK2 expression was abolished as well (Figure S2F). In accordance with the above *in vitro* data using DKK2-treated normal colonic organoids, DKK2 knockout in AKP colon cancer organoids resulted in unchanged expression of the canonical Wnt target genes (Figure 3G). Confocal microscopy and flow cytometry analysis of CTNNB1 in AKP organoids showed that *DKK2* knockout did not alter cellular localization and protein levels of CTNNB1 (Figures S3A and S3B). Moreover, ingenuity pathway analysis of the RNA-seq data from colitis-induced polyps showed marginal reduction of the canonical Wnt signaling pathway activity in the absence of *DKK2* (Figure 3H). These results imply the possibility of the presence of non-canonical DKK2 signaling.

Although the canonical Wnt target genes were unaffected by DKK2 knockout, reduced Lgr5 expression and enhanced differentiation of intestinal epithelial cells are still observed in AKP organoids (Figures 3I and 3J). *LGR5* expression was reduced by random mutations in the *DKK2* gene and the knockout clones showed about three-fold reduction in LGR5 expression compared to the control AKP organoids at day 8 (Figures S2G and S2H). Also, elevation of differentiation marker genes such as *Emp1* and *Slc26a3* was confirmed (Figure 3I). Decreased spheroid/enteroid ratios in morphology reflect reduced stemness in KO organoids as well (Rodriguez-Colman et al., 2017) (Figures 3J and S4A). These data confirmed the necessity of DKK2 in the stemness of colorectal cancer represented by enhanced *LGR5* expression and the underlying mechanisms may not be through the canonical Wnt signaling pathway.

DKK2-driven loss of HNF4α1 protein enhances LGR5 expression in colon cancer cells

Ingenuity pathway analysis (IPA) of the RNA-seq data from colitis-induced polyps suggested a transcription factor, hepatocyte nuclear factor 4-alpha (HNF4A) as an upstream regulator that is activated in the absence of *DKK2* (Figure S5A). HNF4A is a nuclear receptor protein which is crucial for development of the gut (Chen et al., 2019). *Villin*^{CreERT2}-*Hnf4a*$^{fl/fl}$ conditional knockout mice showed destabilization of intestinal epithelium following increased expression of LGR5 upon tamoxifen administration (Cattin et al., 2009). Chellappa et al. have reported the existence of two *Hnf4a* isoforms—*Hnf4α1* and *Hnf4α7*—in the gut epithelium and have discovered the loss of the HNF4α1 isoform in AOM/DSS-driven intestinal tumor cells (Chellappa et al., 2016). Furthermore, inhibition of the *HNF4α1* isoform using shRNA in the Caco2/15 human colon cell line showed reduced ileum villi cells signature and colon differentiated cell signature by gene set enrichment analysis (Babeu et al., 2018). Briefly, loss of HNF4A in colorectal cancer impairs epithelial differentiation.

We tested whether HNF4A is involved in DKK2 downstream signaling in colorectal cancer using AKP and KO organoids. Quantitative gene expression analysis showed that two isoforms of HNF4A, HNF4α1 and HNF4α7, were unchanged in the absence of DKK2 (Figure S5B). On the other hand, the protein level of HNF4α1 was

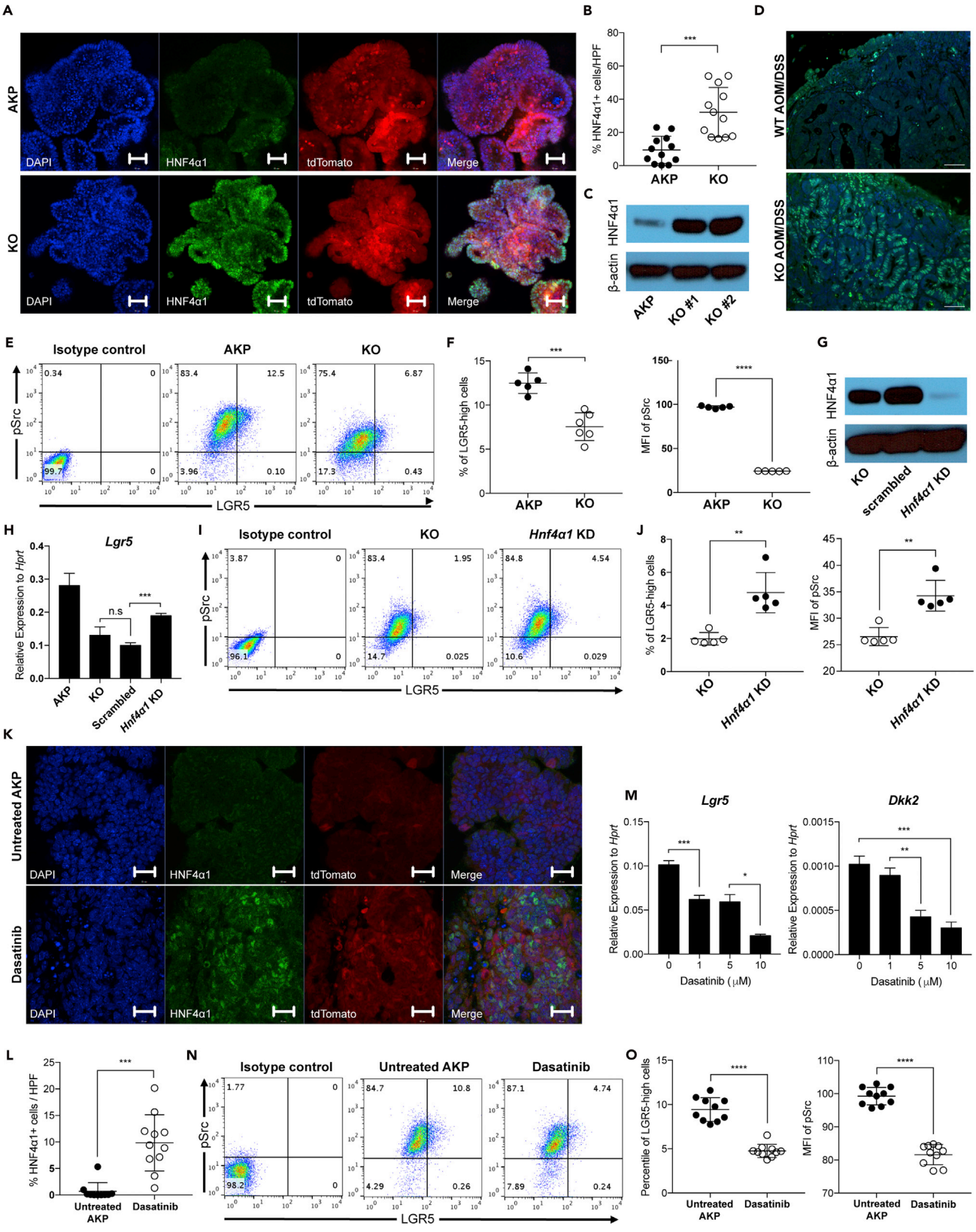
A
AKP
KO
DAPI
HNF4α1
tdTomato
Merge
B
% HNF4α1+ cells/HPF
AKP
KO
C
HNF4α1
β-actin
AKP
KO #1
KO #2
D
WT AOM/DSS
KO AOM/DSS
E
Isotype control
AKP
KO
pSrc
LGR5
F
% of LGR5-high cells
MFI of pSrc
G
KO
scrambled
Hnf4α1 KD
H
Lgr5
Relative Expression to Hprt
n.s
I
Hnf4α1 KD
J
K
Untreated AKP
Dasatinib
L
Untreated AKP
M
Dkk2
Dasatinib (μM)
N
O
Percentile of LGR5-high cells

Figure 4. Loss of HNF4α1 protein mediates DKK2-driven LGR5 expression in colon cancer organoids through proto-oncogene tyrosine-protein kinse Src (c-Src) phosphorylation

(A) Confocal microscopy of HNF4α1 staining in AKP organoids carrying the *tdTomato* reporter gene. Scale bar = 50 μm. KO; *Dkk2* knockout AKP organoids.
(B) Statistical analysis of HNF4α1 positive cells per high power field (HPF) in (A) using ImageJ. Each dot represents a single image of HNF4α1 staining.
(C) Quantification of HNF4α1 in AKP organoids by Western blot analysis. HNF4α1 = 52 kDa, β-actin = 42 kDa.
(D) Representative images of HNF4α1 staining in AOM/DSS-induced tumors from wild type (WT AOM/DSS) and $Villin^{Cre}$-$Dkk2^{fl/fl}$ conditional knockout (KO AOM/DSS) mice. Scale bar = 1 μm.
(E) Flow cytometry analysis of c-Src phosphorylation (pSrc) and LGR5 expression in KO organoids.
(F) Statistic analysis of the percent of cells expressing high levels of LGR5 (LGR5-high: LGR5 and pSrc double-positive) and the mean fluorescence intensity of pSrc in (E).
(G) Quantification of HNF4α1 protein in the HNF4α1 knockdown in DKK2 KO AKP organoids (HNF4α1 KD) by Western blot analysis.
(H) Quantitative gene expression analysis of LGR5 in HNF4α1 KD oragnoids.
(I) Flow cytometry analysis of LGR5 expression and c-Src phosphorylation (pSrc) in HNF4α1 KD.
(J) Statistic analysis of the percent of LGR5-high cells and the mean fluorescence intensity of pSrc in HNF4α1 KD.
(K) Confocal microscopy of HNF4α1 staining in AKP organoids carrying the *tdTomato* reporter gene in the presence or absence of 5 μM of c-Src inhibitor, dasatinib for 48 hr. Scale bar = 20 μm.
(L) Statistic analysis of HNF4α1 positive cells per high power field (HPF) in (K). Each symbol represents a single image of HNF4α1 staining.
(M) Quantitative gene expression analysis of LGR5 and DKK2 in dasatinib treated AKP organoids at 24 hr in a dose-dependent manner.
(N) Flow cytometry analysis of c-Src phosphorylation (pSrc) and LGR5 expression in AKP organoids after 5 μM of dasatinib treatment for 24 hr.
(O) Statistic analysis of LGR5-high cells and pSrc MFI in AKP organoids in (N). *p < 0.05, **p < 0.01, ***p < 0.001, ****p < 0.0001; two-tailed Welch's ttest. Error bars indicate mean ± s.d. Results are representative of three independent experiments.

significantly increased in the nucleus of KO organoids compared to AKP organoids (Figures 4A–4C, S5C, and S5D). This has also been observed in *DKK2* knockout colitis-induced polyps *in vivo* (Figure 4D). The modulation of HNF4α1 protein but not HNF4α1 RNA expression is consistent with a previous report that post-translational modification of HNF4α1 isoform by c-Src leads to proteasomal degradation of HNF4α1 in human colorectal cancer (Chellappa et al., 2012a). We then performed flow cytometry analysis of c-Src phosphorylation and LGR5 expression in colon cancer organoids. *DKK2* knockout in AKP organoids resulted in dramatic reduction of c-Src phosphorylation as well as LGR5 expression followed by decreased numbers of cells expressing high levels of LGR5 (Figures 4E and 4F). Those results indicate that DKK2 is necessary for c-Src-induced proteasomal degradation of HNF4α1, which contributes to LGR5 expression in colon cancer.

To validate the inhibitory effects of HNF4α1 in LGR5 expression in colon cancer, we performed a loss of function study targeting the HNF4α1 gene in KO organoids where the protein level of HNF4α1 was increased by *DKK2* knockout (Figure 4G). Transcriptional expression of *LGR5* was recovered by CRISPR-induced random loss of function mutations in the HNF4α1 gene in KO organoids (Figure 4H). The percentile of cells expressing high levels of LGR5 in KO organoids was also increased by HNF4α1 knockdown (Figures 4I and 4J). Those data confirmed that protein depletion of HNF4α1 by c-Src is a key step in DKK2 downstream signaling for LGR5 expression.

c-Src-induced HNF4α1 phosphorylation has been reported as an underlying mechanism of its degradation in human colorectal cancer cells (Chellappa et al., 2012b). It has been reported that activation of c-Src is sufficient to drive stem cell expansion in intestinal tumorigenesis (Cordero et al., 2014). To validate whether c-Src is the downstream target of DKK2 in the process of HNF4α1 protein degradation, we utilized a well-known c-Src inhibitor, dasatinib in AKP organoid culture. Inhibition of c-Src activation using dasatinib showed increased HNF4α1 protein in the nucleus of AKP organoids similar to what has been shown in KO organoids (Figures 4K and 4L). Reduced transcription of *LGR5* and *DKK2* was observed in dasatinib-treated AKP organoids in a dose-dependent manner (Figure 4M). Flow cytometry analysis of c-Src phosphorylation and LGR5 expression further confirmed that c-Src activation is critical to elevate the number of cells expressing high levels of LGR5 in AKP organoids (Figures 4N and 4O). Following the loss of function study using dasatinib, we performed a gain of function study using recombinant DKK2 protein and normal colonic organoids, which have marginal expression of DKK2. Recombinant DKK2 protein treatment in normal colonic organoid culture increased c-Src phosphorylation about two-fold compared to untreated controls (Figures S6A and S6B). The percentile of LGR5 positive cells in the recombinant DKK2-treated organoids was increased about two-fold as well (Figure S6C). Taken together, our findings suggest DKK2 as an essential factor for the stemness of colorectal cancer represented by enhanced LGR5 expression.

DISCUSSION

Increased expression of the intestinal stem cell marker gene LGR5 is commonly observed in colorectal cancers (Leushacke and Barker, 2012; Szkandera et al., 2015; Li et al., 2016). Recent studies have shown that depletion of

LGR5 expressing cells suppressed metastatic progression of colon cancer in murine model systems (de Sousa e Melo et al., 2017; Fumagalli et al., 2020). Here, we report that DKK2 is required for enhanced LGR5 expression in colorectal cancer. We have confirmed an increased expression of DKK2 in colorectal cancer and identified its positive feedback regulation. DKK2 facilitates c-Src activation followed by proteasomal degradation of the transcription factor HNF4α1. Loss of HNF4α1 elevated LGR5-expressing cancer stem cell populations. These alterations by DKK2 eventually promote colorectal cancer development.

DKK2 is known as a Wnt antagonist in the presence of the receptor Kremen-2 (Wu et al., 2000). Marginal expression of Kremen-2 in colon cancer cells potentiates the agonistic roles of DKK2 in the gut epithelium (Uhlén et al., 2015). Abnormal proliferation of the gut epithelium is often caused by alterations in the β-catenin-induced Wnt canonical pathway (Shtutman et al., 1999). However, proliferation of cancer cells was unchanged in the absence of DKK2 in colitis-induced polyps and colon cancer organoids. We think this is the consequence of functional loss of APC in both colitis-induced tumors and our APC knockout cancer organoids (Fillippo et al., 1998). It permanently activates β-catenin such that the Wnt agonistic or antagonistic functions of DKK2 are minimized in this context. Ingenuity pathway analysis of our RNA-seq data also showed marginal reduction of Wnt/β-catenin signaling in the *DKK2* knockout polyps whereas basal carcinoma signaling was significantly reduced. Expression of the canonical Wnt target genes was unaltered by *DKK2* knockout in APC knockout cancer organoids. Cellular localization and the protein quantity of β-catenin in cancer organoids were unaffected by *DKK2* knockout as well. Collectively, DKK2 effects on the Wnt canonical signaling pathway were not apparent in colonic epithelial cells in the context of functional loss of APC such as colitis-induced tumors.

We showed that DKK2 increased LGR5 expression in colon cancer cells. In the homeostatic condition, intestinal stem cells are primed with Wnt ligands such as Wnt3a for LGR5 expression (Clevers, 2013). In colorectal cancer, a recent study has shown that a transcription factor, GATA6 increases LGR5 expression through repressing BMP4 signaling (Whissell et al., 2014). GATA6 directly bound to the *LGR5* promoter in this report. *DKK2* knockout in AKP organoids increased BMP4 transcription whereas GATA6 expression was unchanged (Figure S5E). Future studies could investigate the molecular mechanisms of DKK2 and HNF4α1 in BMP4-mediated or direct regulation of *LGR5* expression in colorectal cancer.

c-Src activation is commonly observed in aggressive colon cancers and is involved in cell adhesion, invasion, and migration of cancer cells which are essential for metastasis (Lieu and Kopetz, 2010; Cordero et al., 2014; Chen et al., 2014). The underlying mechanisms of c-Src activation in colon cancer cells are still unclear. Our results showed significant reduction of c-Src phosphorylation at Y416 in *DKK2* knockout colon cancer organoids even in the presence of *APC*, *KRAS*, and *TP53* mutations. Gain of function study using recombinant DKK2 further confirmed that DKK2 activates c-Src in normal colonic epithelial cells as well. These findings propose DKK2 as a key upstream regulator of c-Src activation in colonic epithelial cells during tumorigenesis. Further studies to identify the DKK2 receptors in c-Src activation will provide better molecular understanding of the DKK2 downstream signaling pathways.

In this study, we have shown that DKK2 is required for the elevated expression of LGR5 in colon cancer cells through c-Src activation and depletion of HNF4α1. Based on our findings, new therapeutic approaches targeting DKK2 would be beneficial against colorectal cancers, particularly to control LGR5 expressing cancer stem cells.

Limitations of the study

Increased expression of DKK2 is shown in the colitis-induced tumor model and cancer organoids with mutations in *APC*, *KRAS*, *TP53*, and *SMAD4* genes. Based on the pattern of DKK2 expression, this study focused on the roles of DKK2 in colon cancer cells. Further study is needed to understand the roles of DKK2 in the homeostatic condition. In this study, we observed decreased expression of LGR5 by DKK2 knockout in colitis-induced polyps and cancer organoids. LGR5 is expressed in most stem cells including crypt base columnar stem cells and quiescent stem cells and paneth cells as well. A technical limitation of our data is that we cannot provide information about the sub-types of LGR5 expressing stem cells affected by DKK2 knockout.

Resource availability

Lead contact

Further requests for resources should be directed to and will be fulfilled by the lead contact, Alfred L. M. Bothwell (alfred.bothwell@yale.edu).

Materials availability

This study did not generate new materials.

Data and code availability

The accession number for the RNA sequencing data reported in this study is GSE157535.

METHODS

All methods can be found in the accompanying Transparent Methods supplemental file.

SUPPLEMENTAL INFORMATION

Supplemental information can be found online at https://doi.org/10.1016/j.isci.2021.102411.

ACKNOWLEDGMENTS

This work was supported by National Institutes of Health USA, RO1CA168670 (awarded to A.L.M.B).The authors would like to thank GouzelTokmulina and ZuzanaTobiasova for the FACS sorting.

AUTHOR CONTRIBUTIONS

J.S. and A.L.M.B. designed and conducted the experiments, analyzed the data and wrote the manuscript. J.J. performed immunofluorescence and confocal microscopy and Western blot analysis. J.C. and J.L. performed and analyzed RNA-seq experiments. R.K.D. cloned gRNA/Cas9 plasmids targeting DKK2 exon1 and HNF4α1 exon1. J.B. and O.Y. developed colon tumor organoids. J.H. contributed to RNA-seq and quantitative PCR analysis. S.E.M. supported *in vivo* experiments. M.C.A.V. was involved in colonoscopy. W.K., J.K., and J.C. generated recombinant mouse DKK2 protein and polyclonal anti-DKK2 antibody. W.T. and D.W. developed DKK2-floxed mice. H.N.B., R.X.M. and X.L. contributed to immunohistochemistry. J.S. performed all other experiments.

DECLARATION OF INTERESTS

The authors declare no competing interests exist.

Received: October 9, 2020
Revised: January 13, 2021
Accepted: April 6, 2021
Published: May 21, 2021

REFERENCES

Babeu, J.P., Jones, C., Geha, S., Carrier, J.C., and Boudreau, F. (2018). P1 promoter-driven HNF4alpha isoforms are specifically repressed by beta-catenin signaling in colorectal cancer cells. J.Cell Sci. *131*. https://doi.org/10.1242/jcs.214734.

Barker, N., Ridgway, R.A., Van Es, J.H., Van De Wetering, M., Begthel, H., Van Den Born, M., Danenberg, E., Clarke, A.R., Sansom, O.J., and Clevers, H. (2009). Crypt stem cells as the cells-of-origin of intestinal cancer. Nature *457*, 608–611.

Barker, N., Van Es, J.H., Kuipers, J., Kujala, P., Van Den Born, M., Cozijnsen, M., Haegebarth, A., Korving, J., Begthel, H., Peters, P.J., and Clevers, H. (2007). Identification of stem cells in small intestine and colon by marker gene Lgr5. Nature *449*, 1003–1007.

Bray, F., Ferlay, J., Soerjomataram, I., Siegel, R.L., Torre, L.A., and Jemal, A. (2018). Global cancer statistics 2018: GLOBOCAN estimates of incidence and mortality worldwide for 36 cancers in 185 countries. CA Cancer J. Clin. *68*, 394–424.

Cattin, A.L., Le Beyec, J., Barreau, F., Saint-Just, S., Houllier, A., Gonzalez, F.J., Robine, S., Pincon-Raymond, M., Cardot, P., Lacasa, M., and Ribeiro, A. (2009). Hepatocyte nuclear factor 4alpha, a key factor for homeostasis, cell architecture, and barrier function of the adult intestinal epithelium. Mol.Cell. Biol. *29*, 6294–6308.

Chellappa, K., Deol, P., Evans, J.R., Vuong, L.M., Chen, G., Briancon, N., Bolotin, E., Lytle, C., Nair, M.G., and Sladek, F.M. (2016). Opposing roles of nuclear receptor HNF4alpha isoforms in colitis and colitis-associated colon cancer. Elife *5*. https://doi.org/10.7554/eLife.10903.

Chellappa, K., Jankova, L., Schnabl, J.M., Pan, S., Brelivet, Y., Fung, C.L., Chan, C., Dent, O.F., Clarke, S.J., Robertson, G.R., and Sladek, F.M. (2012a). Src tyrosine kinase phosphorylation of nuclear receptor HNF4alpha correlates with isoform-specific loss of HNF4alpha in human colon cancer. Proc. Natl. Acad. Sci. U S A *109*, 2302–2307.

Chellappa, K., Jankova, L., Schnabl, J.M., Pan, S., Brelivet, Y., Fung, C.L.S., Chan, C., Dent, O.F., Clarke, S.J., Robertson, G.R., and Sladek, F.M. (2012b). Src tyrosine kinase phosphorylation of nuclear receptor HNF4 correlates with isoform-specific loss of HNF4 in human colon cancer. Proc.Natl.Acad.Sci. U S A *109*, 2302–2307.

Chen, J., Elfiky, A., Han, M., Chen, C., and Saif, M.W. (2014). The role of Src in colon cancer and its therapeutic implications. Clin. Colorectal Cancer *13*, 5–13.

Chen, L., Toke, N.H., Luo, S., Vasoya, R.P., Aita, R., Parthasarathy, A., Tsai, Y.H., Spence, J.R., and Verzi, M.P. (2019). HNF4 factors control chromatin accessibility and are redundantly required for maturation of the fetal intestine. Development *146*, dev179432.

Clevers, H. (2013). The intestinal crypt, a prototype stem cell compartment. Cell *154*, 274–284.

Cordero, J.B., Ridgway, R.A., Valeri, N., Nixon, C., Frame, M.C., Muller, W.J., VIDAL, M., and SANSOM, O.J. (2014). c-Src drives intestinal

regeneration and transformation. EMBO J. *33*, 1474–1491.

de Sousa e Melo, F., Kurtova, A.V., Harnoss, J.M., Kljavin, N., Hoeck, J.D., Hung, J., Anderson, J.E., Storm, E.E., Modrusan, Z., Koeppen, H., et al. (2017). A distinct role for Lgr5(+) stem cells in primary and metastatic colon cancer. Nature *543*, 676–680.

Drost, J., and Clevers, H. (2018). Organoids in cancer research. Nat. Rev. Cancer *18*, 407–418.

Fillippo, C.D., Carderni, G., Bazzicalupo, M., Briani, C., Giannini, A., Fazi, M., and Dolaral, P. (1998). Mutations of the Apc gene in experimental colorectal carcinogenesis induced by azoxymethane in F344 rats. Br. J. Cancer *77*, 2148–2151.

Fumagalli, A., Oost, K.C., Kester, L., Morgner, J., Bornes, L., Bruens, L., Spaargaren, L., Azkanaz, M., Schelfhorst, T., Beerling, E., et al. (2020). Plasticity of Lgr5-negative cancer cells drives metastasis in colorectal cancer. Cell Stem Cell *26*, 569–578.e7.

Gregorieff, A., Pinto, D., Begthel, H., Destree, O., Kielman, M., and Clevers, H. (2005). Expression pattern of Wnt signaling components in the adult intestine. Gastroenterology *129*, 626–638.

Leushacke, M., and Barker, N. (2012). Lgr5 and Lgr6 as markers to study adult stem cell roles in self-renewal and cancer. Oncogene *31*, 3009–3022.

Li, X.B., Yang, G., Zhu, L., Tang, Y.L., Zhang, C., Ju, Z., Yang, X., and Teng, Y. (2016). Gastric Lgr5(+) stem cells are the cellular origin of invasive intestinal-type gastric cancer in mice. Cell Res *26*, 838–849.

Lieu, C., and Kopetz, S. (2010). The SRC family of protein tyrosine kinases: a new and promising target for colorectal cancer therapy. Clin. Colorectal Cancer *9*, 89–94.

Mao, B., and Niehrs, C. (2003). Kremen2 modulates Dickkopf2 activity during Wnt/lRP6 signaling. Gene *302*, 179–183.

Matano, M., Date, S., Shimokawa, M., Takano, A., Fujii, M., Ohta, Y., Watanabe, T., Kanai, T., and Sato, T. (2015). Modeling colorectal cancer using CRISPR-Cas9-mediated engineering of human intestinal organoids. Nat. Med. *21*, 256–262.

Matsui, A., Yamaguchi, T., Maekawa, S., Miyazaki, C., Takano, S., Uetake, T., Inoue, T., Otaka, M., Otsuka, H., Sato, T., et al. (2009). DICKKOPF-4 and -2 genes are upregulated in human colorectal cancer. Cancer Sci. *100*, 1923–1930.

Niehrs, C. (2006). Function and biological roles of the Dickkopf family of Wnt modulators. Oncogene *25*, 7469–7481.

Phelps, R.A., Broadbent, T.J., Stafforini, D.M., and Jones, D.A. (2009). New perspectives on APC control of cell fate and proliferation in colorectal cancer. Cell Cycle *8*, 2549–2556.

Rodriguez-Colman, M.J., Schewe, M., Meerlo, M., Stigter, E., Gerrits, J., Pras-Raves, M., Sacchetti, A., Hornsveld, M., Oost, K.C., Snippert, H.J., et al. (2017). Interplay between metabolic identities in the intestinal crypt supports stem cell function. Nature *543*, 424–427.

Sato, T., Vries, R.G., Snippert, H.J., Van De Wetering, M., Barker, N., Stange, D.E., Van Es, J.H., Abo, A., Kujala, P., Peters, P.J., and Clevers, H. (2009). Single Lgr5 stem cells build crypt-villus structures in vitro without a mesenchymal niche. Nature *459*, 262–265.

Schepers, A.G., Snippert, H.J., Stange, D.E., Van Den Born, M., Van Es, J.H., Van De Wetering, M., and Clevers, H. (2012). Lineage tracing reveals Lgr5+ stem cell activity in mouse intestinal adenomas. Science *337*, 730–735.

Shtutman, M., Zhurinsky, J., Simcha, I., Albanese, C., D'amico, M., Pestell, R., and Ben-Ze'ev, A. (1999). The cyclin D1 gene is a target of the b-catenin LEF-1 pathway. Proc. Natl. Acad. Sci. U S A *96*, 5522–5527.

Szkandera, J., Herzog, S., Pichler, M., Stiegelbauer, V., Stotz, M., Schaberl-Moser, R., Samonigg, H., Asslaber, M., Lax, S., Leitner, G., et al. (2015). LGR5 rs17109924 is a predictive genetic biomarker for time to recurrence in patients with colon cancer treated with 5-fluorouracil-based adjuvant chemotherapy. Pharmacogenomics J. *15*, 391–396.

Uhlén, M., Fagerberg, L., Hallström, B.M., Lindskog, C., Oksvold, P., Mardinoglu, A., Sivertsson, Å., Kampf, C., Sjöstedt, E., Asplund, A., et al. (2015). Tissue-based map of the human proteome. Science *347*, 1260419.

Vogelstein, B., Fearon, E.R., Hamilton, S.R., Kern, S.E., Preisinger, A.C., Leppert, M., Nakamura, Y., White, R., Smits, A.M., and Bos, J.L. (1988). Genetic alteration during colorectal-tumor development. N. Engl. J. Med. *319*, 525–532.

Vogelstein, B., Papadopoulos, N., Velculescu, V.E., Zhou, S., Diaz, L.A., JR., and Kinzler, K.W. (2013). Cancer genome landscape. Science *339*, 1546–1558.

Whissell, G., Montagni, E., Martinelli, P., Hernando-Momblona, X., Sevillano, M., Jung, P., Cortina, C., Calon, A., Abuli, A., and Castells, A. (2014). The transcription factor GATA6 enables self-renewal of colon adenoma stem cells by repressing BMP gene expression. Nat.Cell Biol. *16*, 695–707.

Wu, W., Glinka, A., Delius, H., and Niehrs, C. (2000). Mutual antagonism between dickkopf1 and dickkopf2 regulates Wnt:β-catenin signalling. Curr. Biol. *10*, 1611–1614.

iScience, Volume *24*

Supplemental information

Dickkopf-2 regulates the stem cell marker LGR5 in colorectal cancer via HNF4α1

Jae Hun Shin, Jaekwang Jeong, Jungmin Choi, Jaechul Lim, Ravi K. Dinesh, Jonathan Braverman, Jun Young Hong, Stephen E. Maher, Maria C. Amezcua Vesely, WonJu Kim, Ja-Hyun Koo, Wenwen Tang, Dianqing Wu, Holly N. Blackburn, Rosa M. Xicola, Xavier Llor, Omer Yilmaz, Je-Min Choi, and Alfred L.M. Bothwell

Supplemental figures and legends

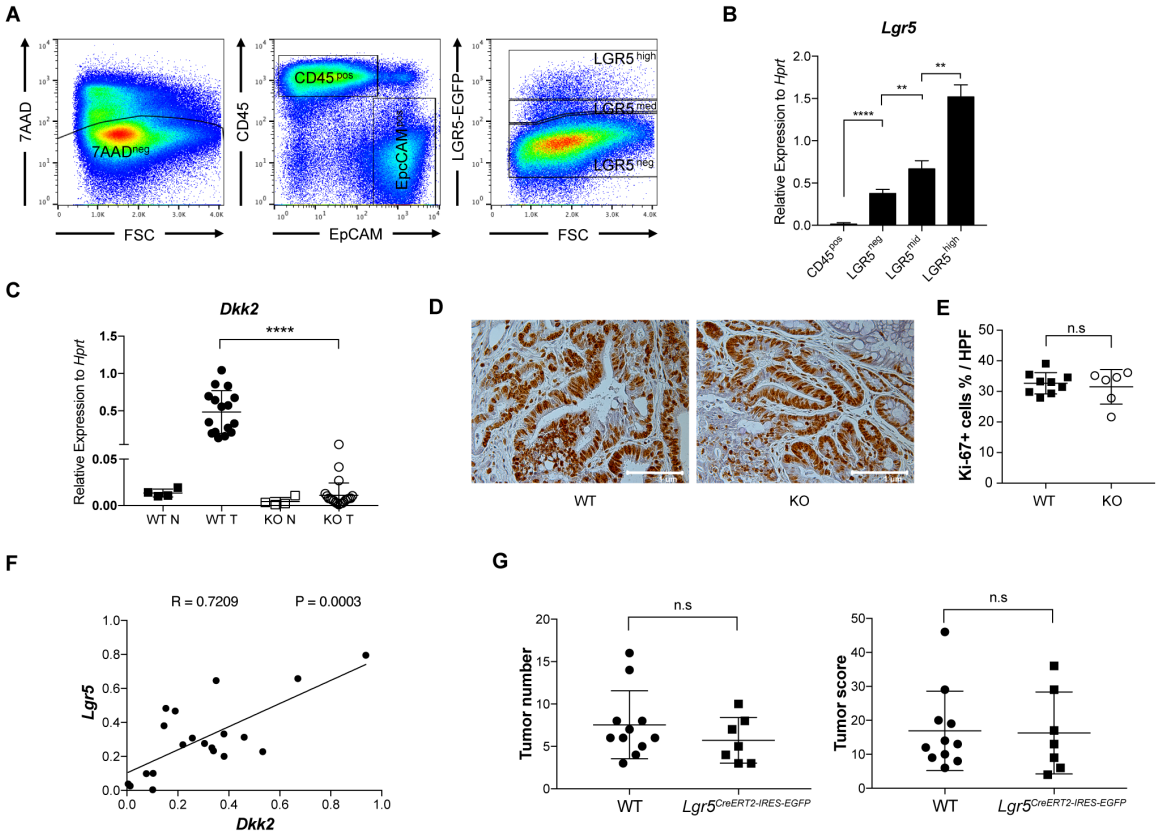

Figure S1. *Lgr5* expression and *Dkk2* knockout phenotype in the colitis-induced tumor model using V*illin*^{Cre}-*Dkk2*$^{fl/fl}$ and tamoxifen-inducible *Lgr5*^{CreERT2}-*Dkk2*$^{fl/fl}$ knockout mice (Related to Figures 1 and 2). (A) Sorting strategy for tumor-infiltrating lymphocytes (CD45^{pos}EpCAM^{neg}), differentiated epithelial cells (CD45^{neg}EpCAM^{pos}LGR5-EGFP^{neg}), Paneth-like cells and transit amplifying cell (CD45^{neg}EpCAM^{pos}LGR5-EGFP^{mid}) and stem cells (CD45^{neg}EpCAM^{pos}LGR5-EGFP^{high}) in colitis-induced tumors. Each population was sorted from the 7AAD negative live cell population. **(B)** Quantitative *Lgr5* expression analysis in the sorted cells. **(C)** Quantitative gene expression analysis of *Dkk2* in tumor tissues from AOM/DSS-treated *Villin*^{Cre}-*Dkk2*$^{fl/fl}$ knockout mice. WT N: wild type normal colon, *n*=4, WT T: wild type tumor, *n*=16, KO N: *Dkk2* knockout normal colon, *n*=4, KO T: *Dkk2* knockout tumor, *n*=20. **(D and E)** Proliferation analysis of AOM/DSS-induced tumors by Ki-67 staining (D) and statistical analysis (E). **(F)** Expressional correlation of *Dkk2* and *Lgr5* in collected tumor tissues in WT and tamoxifen-inducible KO mice. Each dot represents an individual tumor tissue. Pearson r test. **(G)**

Tumor number and score in *Lgr5*$^{CreERT2\text{-}IRES\text{-}EGFP}$ mice (Lgr5, *n*=7) having loss of one *Lgr5* allele by insertion of the *Lgr5*$^{CreERT2\text{-}IRES\text{-}EGFP}$ transgene compared to wild type C57BL/6 (WT, *n*=11) mice after AOM/DSS treatment. n.s, not significant, **P<0.01, ***P<0.001, ****P<0.0001, error bars represent ± s.d.; two-tailed Welch's t-test. *n* represents the number of independent animals.

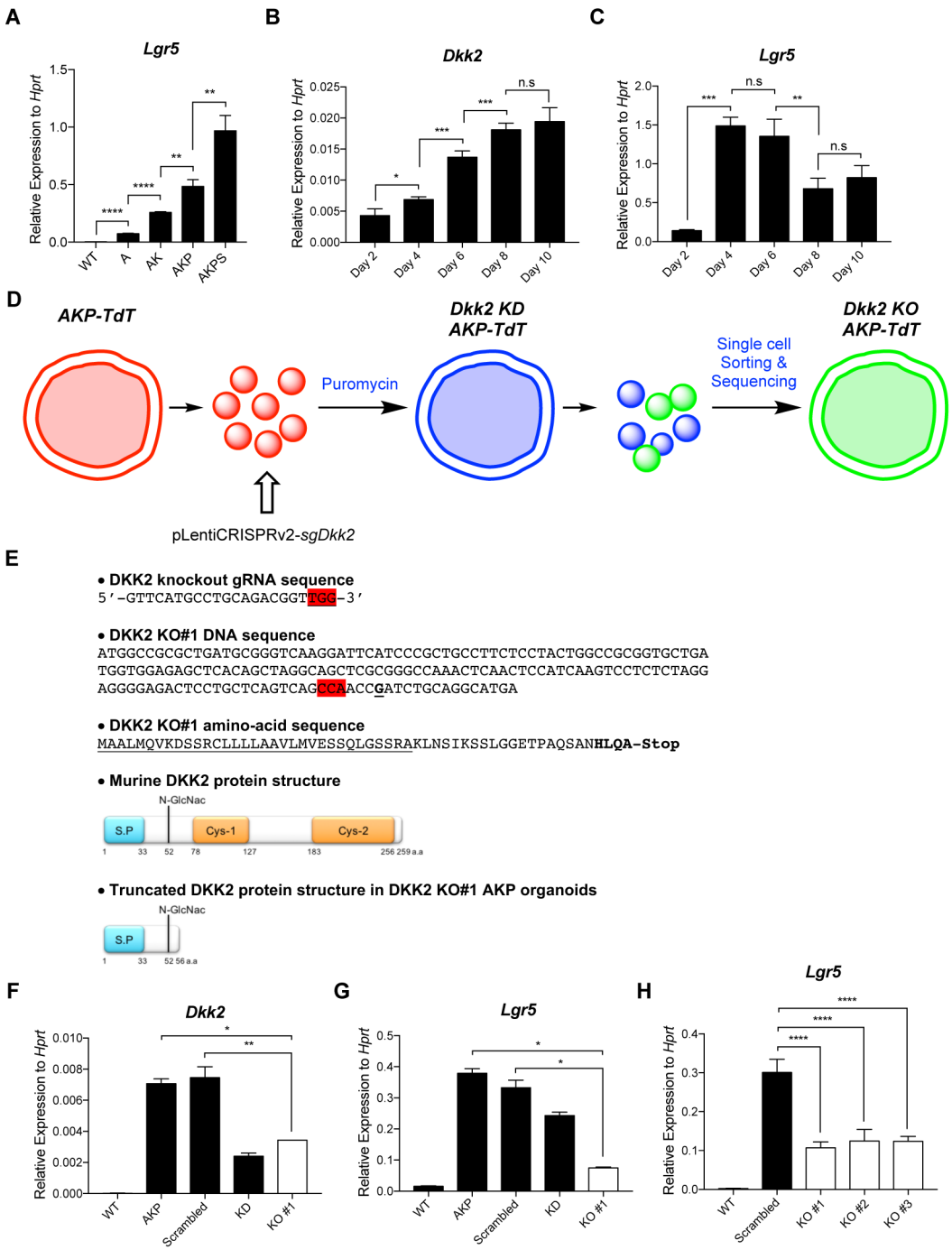

Figure S2. Generation of *Dkk2* knockout colon cancer organoids (Related to Figure 3). (A) Quantitative PCR analysis of *Lgr5* expression in colonic organoids carrying various mutations. Wild type organoids were cultured in the WERN medium containing Wnt3a, EGF, Rspondin1 and Noggin. *Apc* only mutant organoids were grown in the EGF only containing medium. *Apc, Kras, Tp53* and *Smad4* double, triple and quadruple mutant organoids culture used the minimal

medium without all of those four growth factors. WT; wild type normal colonic organoids, A; *Apc knockout* organoids, AK; *Apc knockout-Kras*^{G12D} mutant organoids, AKP; *Apc knockout-Kras*^{G12D}-*Tp53* knockout mutant organoids. AKPS; *Apc knockout-Kras*^{G12D}*-Tp53 knockout-Smad4 knockout* mutant organoids. **(B-C)** Expression of *Dkk2* and *Lgr5* in AKP triple mutant organoids was analyzed in a time-dependent manner. **(D)** A schematic diagram of the development of *Dkk2* knockout AKP organoids. Isolated AKP organoid cells were transduced with lentivirus carrying *Dkk2* guide RNA, Cas9 and Puromycin resistant genes. Transduced *Dkk2* knockdown (KD) cells were selected in the presence of Puromycin. The selected cells were sorted as a single cell then cloned. Each *Dkk2* knockout (KO) clone was identified by sequencing genomic DNA. **(E)** Sequence of guide RNA targeting *Dkk2* exon1. Representative genomic DNA sequence and amino-acid sequence of DKK2 in the knockout AKP organoids. KO clone #1 is shown. Frame shift mutation in *Dkk2* exon1 resulted in a truncated DKK2 protein (Red box; PAM sequence. G was omitted. 1-33 S.P; signal peptide. 34-56; truncated 23 amino acids, **HLQA-Stop**; newly generated sequence by frame shift mutation). Normal and truncated DKK2 protein structures are displayed. **(F-H)** Organoids were dispersed as single or 2-3 attached cells by TrypLE enzyme digestion. The isolated cells were suspended in matrigel. Once matrigel solidified, the AKP organoid culture medium was added. The culture medium was replaced every other day. Quantitative PCR analysis of *Dkk2* and *Lgr5* expression in KO organoids at day 8 after plating isolated single organoid cells (F and G). 3 independent KO clones are shown for *Lgr5* expression (H). WT; wild type colonic organoids cultured in the WERN medium, AKP; Untreated AKP organoids, Scrambled; Scrambled guide RNA transduced AKP organoids, KO; unsorted polyclonal *Dkk2* knockout organoids, KO with #; sorted *Dkk2* knockout organoid clones. n.s, not significant, *P < 0.05, **P<0.01, ***P<0.001, ****P<0.0001; two-tailed Welch's t-test. Error bars indicate mean ± s.d. Results are representative of two identical independent experiments.

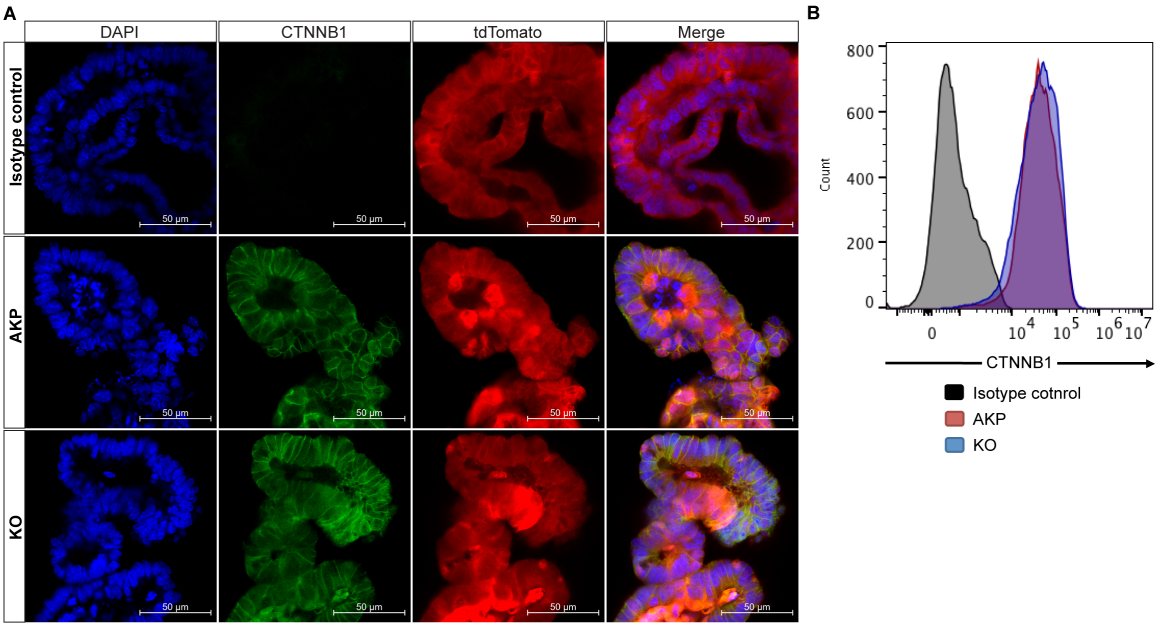

Figure S3. Analysis of CTNNB1 protein in *Dkk2* knockout AKP organoids (Related to Figure 3). (A) Confocal microscopy analysis of CTNNB1 in control (AKP) and *Dkk2* knockout (KO) AKP organoids. Scale bar = 5 µm. **(B)** Quantification of CTNNB1 protein in control (red) and *Dkk2* knockout (blue) AKP organoid cells at day 3 after plating isolated single organoid cells by intracellular staining flow cytometry analysis. Results are representative of at least three biological replicates.

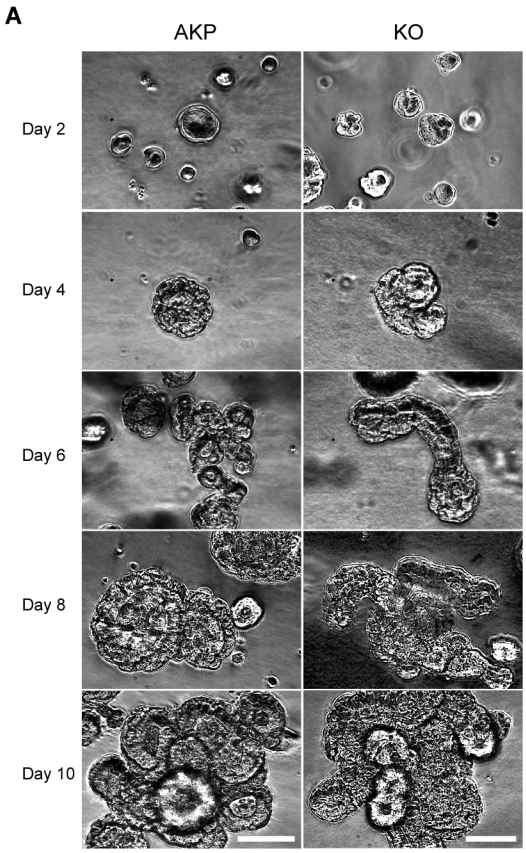

Figure S4. Morphology of AKP organoids (Related to Figure 3). (A) Images were captured at the indicated time points after plating the isolated cells for 10 days. Control AKP organoids formed multi-circular morphology whereas *Dkk2* knockout AKP organoids showed linearized and entangled morphology. Scale bar = 5 μm.

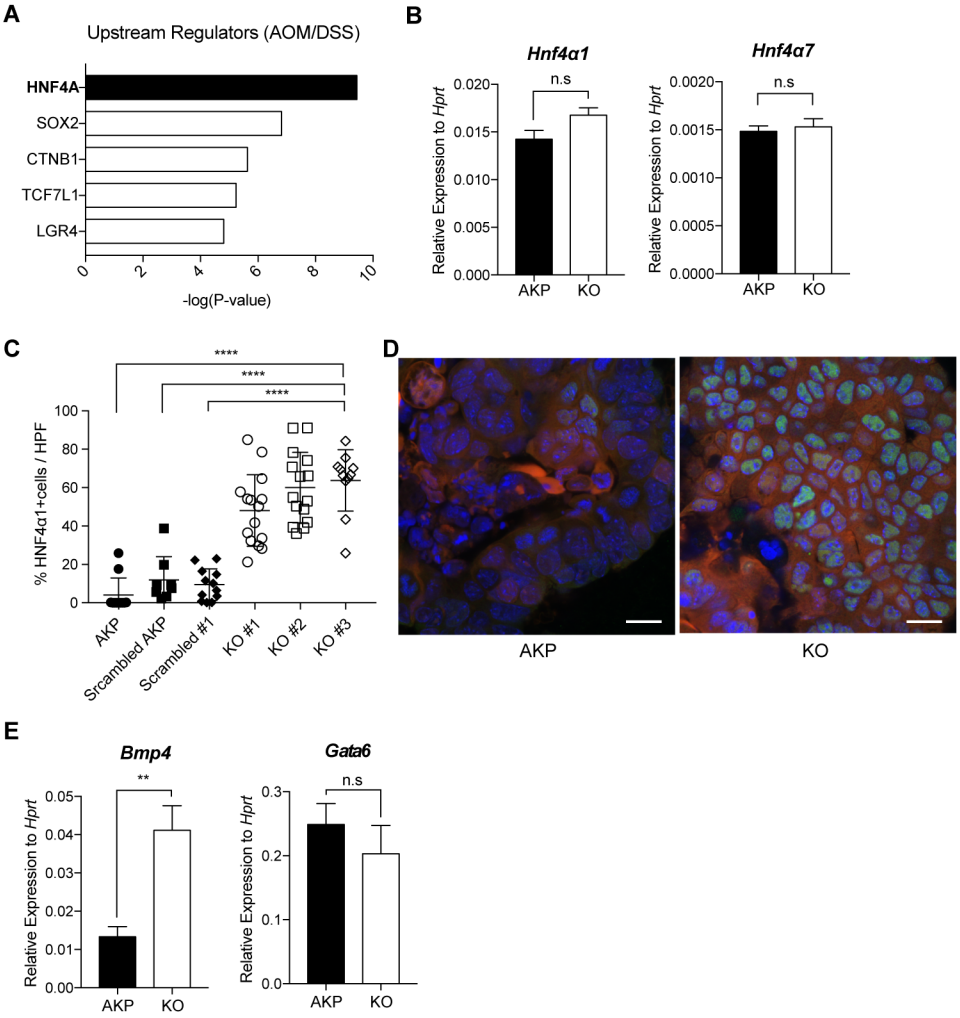

Figure S5. mRNA and protein levels of HNF4α1 in Dkk2 knockout AKP organoids (Related to Figure 4). (A) Ingenuity pathway analysis suggested upstream regulators in the absence of *Dkk2* from AOM/DSS-treated colitis induced polyps. **(B and E)** Quantitative gene expression analyses of *Hnf4a* isoforms (B) and *Bmp4 and Gata6* (E) on day 8 after passaging control (AKP) or *Dkk2* knockout AKP (KO) organoids. **(C and D)** Confocal microscopy of HNF4α1 protein in AKP organoids. Statistical analysis of HNF4α1 positive cells in 3 independent *Dkk2* knockout (KO) AKP organoid clones (C). n.s = not significant, *P<0.05, **P<0.01, ***P<0.001, ****P<0.0001; two tailed Welch's t test. Error bars represent ± s.d. HPF, high power field. Scrambled, scrambled guide RNA transduction. Numbers (#1-3) indicate the clones. Each *symbol* represents a single image of HNF4α1 staining. Results are representative of two identical independent experiments. Representative images of HNF4α1 staining in wild type and *Dkk2*

knockout AKP organoids with higher magnification (D). Green; HNF4α1, Red; tdTomato, Blue; DAPI, Scale bar = 2 μm.

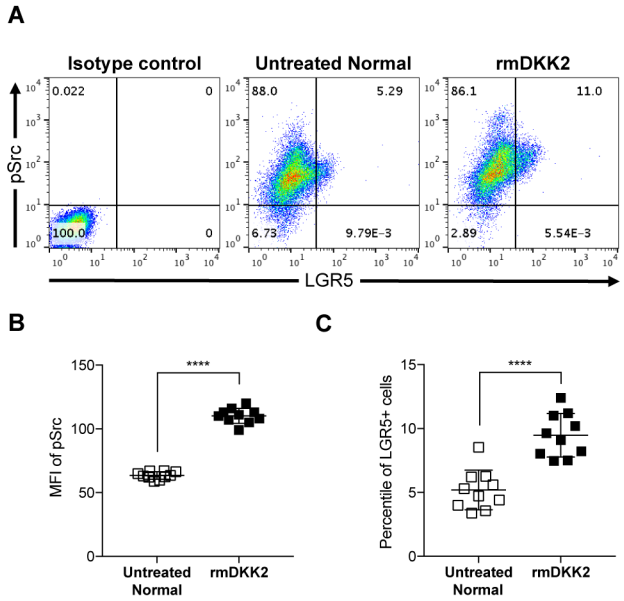

Figure S6. DKK2-induced phosphorylation of c-Src in normal colonic organoids (Related to Figure 4).

(A) Flow cytometry analysis of phosphorylated c-Src (pSrc) and LGR5 expression in normal colonic organoids in the presence of 1 μg/ml of recombinant mouse DKK2 (rmDKK2) protein for 12 h. **(B)** Statistic analysis of the mean fluorescence intensity (MFI) of pSrc in (A). **(C)** Statistic analysis of the percentile of LGR5 positive stem cells in normal colonic organoids in (A). ****P<0.0001; two-tailed Welch's t-test. Error bars indicate mean ± s.d. Results are representative of three independent experiments. Each *symbol* represents an independent sample in each group.

Table S1. The list of quantitative PCR primers (Related to Figures 1-4).

Bmi1	F	ATCCCCACTTAATGTGTGTCCT
	R	CTTGCTGGTCTCCAAGTAACG
BMP4	F	TTCCTGGTAACCGAATGCTGA
	R	CCTGAATCTCGGCGACTTTTT

DKK2	F	GTACCCGCTGCAATAATGGAATCT
	R	ATCCCAGGTCATGGTTGGAATAGT
Emp1	F	TTGGTGCTACTGGCTGGTCT
	R	CATTGCCGTAGGACAGGGAG
FoxM1	F	CTGATTCTCAAAAGACGGAGGC
	R	TTGATAATCTTGATTCCGGCTGG
GATA6	F	TTGCTCCGGTAACAGCAGTG
	R	GTGGTCGCTTGTGTAGAAGGA
HNF4α1	F	ATGCGACTCTCTAAAACCCTTG
	R	ACCTTCAGATGGGGACGTGT
HNF4α7	F	TCCTTATGCCCTCACAGGGT
	R	TGGTCCTATGGGGTCACACA
HPRT	F	CTCCTCAGACCGCTTTTTGC
	R	TCATCGCTAATCACGACGCT
mKi67	F	ATCATTGACCGCTCCTTTAGGT
	R	GCTCGCCTTGATGGTTCCT
Krt20	F	AGTTTTCACCGAAGTCTGAGTTC
	R	GTAGCTCATTACGGCTTTGGAG
LEF1	F	TGTTTATCCCATCACGGGTGG
	R	CATGGAAGTGTCGCCTGACAG
Lgr5	F	GGGAGCGTTCACGGGCCTTC
	R	GGTTGGCATCTAGGCGCAGGG
Myc	F	CCCTATTTCATCTGCGACGAG
	R	GAGAAGGACGTAGCGACCG
RNF43	F	CCGGGTCATTTCGTGCCTC
	R	CCTGGTTCCTGGTAAGATGGAG
Slc26a3	F	GCCGTGGTTGGGAACATGA

	R	GCAAATCCTTTGAATGCTCCAG
TCF1	F	AGCTTTCTCCACTCTACGAACA
	R	AATCCAGAGAGATCGGGGGTC
TCF4	F	CGAAAAGTTCCTCCGGGTTTG
	R	CGTAGCCGGGCTGATTCAT
Tert	F	GCACTTTGGTTGCCCAATG
	R	GCACGTTTCTCTCGTTGCG
ZnRf3	F	GGCGACTATACCACCCACAC
	R	CTTCACCACTCCTACCCAGC

Transparent Methods

Key Resources Table

REAGENT OR RESOURCE	SOURCE	IDENTIFIER
Antibodies		
Anti-DKK2 antibody (polyclonal)	Millipore Sigma	Cat# 06-1087, RRID:AB_10806082
Rabbit normal IgG control antibody	Millipore Sigma	Cat# 12-370, RRID:AB_145841
Ki-67 Monoclonal Antibody (Clone SolA15)	Thermo Fisher Scientific	Cat# 14-5698-82, RRID:AB_10854564
Anti-phospho-Src (Ty416) antibody (Clone 9A6)	Millipore Sigma	Cat# 05-677, RRID:AB_309898
Mouse IgG3 Isotype control	Thermo Fisher Scientific	Cat# 14-4742-82, RRID:AB_470120
BV421 Rat anti-mouse IgG3 antibody (Clone R40-82)	BD Biosciences	Cat# 565808, RRID:AB_2739364
Anti-HNF4a1 antibody (Clone K9218)	R&D Systems	Cat# PP-K9218-00, RRID:AB_2116902
Mouse IgG2A Isotype control	R&D Systems	Cat# MAB003, RRID:AB_357345
Goat anti-mouse IgG2a secondary antibody, Alexa Fluor 488	Thermo Fisher Scientific	Cat# A-21131, RRID:AB_2535771
LGR5 mouse monoclonal antibody (Clone 2A2 Dylight488 conjugated)	OriGene	Cat# TA400002; RRID:AB_2622395
Mouse IgG1 Isotype Control, Dylight488 conjugate antibody	Thermo Fisher Scientific	Cat# MA1-191-D488, RRID:AB_2536927
PE-Cyanine7 Anti-Mouse CD45 (Clone 30-F11) antibody	Tonbo Biosciences	Cat# 60-0451, RRID:AB_2621848
CD326 (EpCAM) Monoclonal Antibody (Clone G8.8, APC)	Thermo Fisher Scientific	Cat# 17-5791-80, RRID:AB_2734965
CD16/32 Monoclonal Antibody (Clone 93)	Thermo Fisher Scientific	Cat# 14-0161-82, RRID:AB_467133
Chemicals Peptides and Recombinant proteins		
Azoxymethane	Sigma-Aldrich	Cat# A5486

DEXTRAN SULFATE SODIUM SALT (36,000-50,000 M.Wt.) MP Grade	MP Biomedicals	Cat# 0216011080
Tamoxifen	Sigma-Aldrich	Cat# T5648
Sunflower seed oil from Helianthus annuus	Sigma-Aldrich	Cat# S5007
Recombinant mouse DKK2 protein	R&D Systems	Cat# 2435-DKB-010
Puromicyn	Sigma-Aldrich	Cat# P9620
Blasticidin	Sigma-Aldrich	Cat# 15205
Dasatinib	Sigma-Aldrich	Cat# CDS023389
Recombinant murine EGF	Peprotech	Cat# 315-09
Nutlin-3	Cayman	Cat# 10004372
PEG-itTM Virus Precipitation Solution	SBI	Cat# LV810A-1
Hexadimethrine bromide (Polybrene)	Sigma-Aldrich	Cat# H9268
Y-27632	Tocris	Cat# 1254
B-27® Supplement (50X), minus vitamin A	Thermo Fisher Scientific	Cat# 12587010
N-2 Supplement (100X)	Thermo Fisher Scientific	Cat# 17502048
Advanced DMEM/F-12	Thermo Fisher Scientific	Cat# 12634010
TrypLE™ Express Enzyme (1X)	Gibco	Cat# 12605010
Corning® Matrigel® Growth Factor Reduced (GFR) Basement Membrane Matrix, Phenol Red-free	Corning	Cat# 356231
GlutaMAX™ Supplement	Gibco	Cat# 35050061
Collagenase IV	Worthington Biochemical	Cat# LS004188
Dispase II, protease	Sigma-Aldrich	Cat# D4693
16% Paraformaldehyde (PFA) solution, EM grade	Thermo Fisher Scientific	Cat# 50-980-488
Normal Goat Serum (10%)	KPL	Cat# 71-00-27
Glycogen, RNA grade	Thermo Fisher Scientific	Cat# R0551
TRIzol Reagent	Thermo Fisher Scientific	Cat# 15596018
Zombie Aqua™ Fixable Viability Kit	Biolegend	Cat# 423102

Critical Commercial Assays		
Foxp3 / Transcription Factor Staining Buffer Set	Thermo Fisher Scientific	Cat#00-5523-00
RNeasy kit	QIAGEN	Cat#74106
miRNeasy kit	QIAGEN	Cat#217004
Illumina TruSeq stranded mRNA preparation kits	Illumina	Cat#20020594/20020595
IntestiCultTM Organoid Growth Medium (Mouse)	Stemcell	Cat# 06005
DAB Peroxidase HRP Substrate Kit (with Nickel), 3,3'-diaminobenzidine	VECTOR Laboratories	Cat# SK-4100
R.T.U. elite ABC Reagent	VECTOR Laboratories	Cat# PK-7100
ProLong™ Gold Antifade Mountant with DAPI	Thermo Fisher Scientific	Cat# P36941
SuperSignal™ West Femto Maximum Sensitivity Substrate	Thermo Fisher Scientific	Cat# 34904

Experimental Models: Organisms/Strains		
Mouse: C57BL/6J	The Jackson Laboratory	JAX:000664
Mouse: Villin$^{Cre+/-}$-DKK2$^{fl/fl}$	This paper	N/A
Mouse: Lgr5$^{CreERT2\text{-}IRES\text{-}EGFP}$-DKK2$^{fl/fl}$	This paper	N/A
Sequence-Based Reagents		
Primers for qPCR, A table attached below	This paper	N/A
sgRNA for CRISPR gene editing, A table attached below	This paper	N/A
Software and Algorithms		
FlowJo v10.5	Tree Star	RRID:SCR_008520
GraphPad Prism 7.0	GraphPad Software	RRID:SCR_002798
ZEN Digital Imaging Light Microscopy	Zeiss	RRID:SCR_013672
Image J	NIH	RRID:SCR_003070
Bruker MS FX PRO software	Bruker	RRID:SCR_017365
IPA 48207413	QIAGEN	RRID:SCR_008653
TopHat v2.1.0	Johns Hopkins University CCB	RRID:SCR_013035
HTSeq v0.8.0	HTSeq	RRID:SCR_005514
DESeq v2	Bioconductor	RRID:SCR_000154
Recombinant DNA		
LentiCRISPR v2	Addgene	Cat# 52961
LentiCRISPR v2-Blast	Addgene	Cat# 83480
Other		
8-well Chamber Slide w/ removable wells	Thermo Fisher Scientific	Cat# 154534PK
Lysing Matrix D, 2 mL Tube	MP Biomedicals	Cat# 116913-100

Animals

All studies handling animals were approved by institutional animal care and use committee at the Yale University School of Medicine animal facility. *Dkk2$^{fl/fl}$* mice were developed by following procedures. A targeting vector was designed to insert a loxP site upstream of Exon 2 of the *Dkk2* gene, followed by *a frt-flanked neomycin resistance (neo)* cassette. An additional *loxP* site was added downstream of Exon 3. The construct was electroporated into 129 embryonic stem (ES) cells, and correctly targeted ES cells were injected into blastocysts. Chimeric males were bred with C57BL/6 females, and their offspring were bred with *ROSA26-Flpe* mice to remove the *PGKneo* cassette. Resulting *Dkk2-floxed* mice were crossed to remove the *Flp*-expressing allele, and subsequently backcrossed to C57BL/6N mice for more than 5 generations. *Lgr5$^{CreERT2\text{-}IRES\text{-}}$*

^{EGFP} mice were gifted from Dr. Richard Flavell. *Villin*^{Cre} mice were gifted from Dr. Ruslan Medzhitov. The *Villin*^{Cre} and *Lgr5*$^{CreERT2\text{-}IRES\text{-}EGFP}$ mice were crossed with *Dkk2*$^{fl/fl}$ mice to generate conditional *Dkk2* knockout mice.

Colitis-induced tumor model

12.5 mg/kg of azoxymethane (AOM, Sigma, A5486) was administered to 6-8 weeks old *Villin*$^{Cre/+}$-*Dkk2*$^{fl/fl}$ or *Lgr5*$^{CreERT2\text{-}IRES\text{-}EGFP/+}$-*Dkk2*$^{fl/fl}$ mice via intra-peritoneal injection. *Villin*$^{+/+}$-*Dkk2*$^{fl/fl}$ or *Lgr5*$^{+/+}$-*Dkk2*$^{fl/fl}$ littermate mice were used as controls. Both male and female mice were subjected and the number of gender was matched in experimental and control groups. After 5 days, mice were treated with 2.5 % of dextran sodium sulfate (DSS, MP biomedicals, molecular mass 36,000–50,000 Da) in the drinking water for 5 days followed by 14 days of regular water. This cycle was performed three times. 7 days after DSS treatment in each cycle, 200 μl of tamoxifen (10 mg/ml in sunflower oil, Sigma, T5648) was delivered into *Lgr5*$^{CreERT2\text{-}IRES\text{-}EGFP/+}$-*Dkk2*$^{fl/fl}$ mice and their littermate controls by intra-peritoneal injection every other day, total three injections per DSS cycle.

Endoscopy

Colonoscopy was performed using the Coloview system (Karl Storz) following the manufacturer's protocol. Mice were anaesthetized by isoflurane. Total number and sizes of tumors were recorded during colonoscopy in a blinded fashion. Tumor sizes were scored from 0 to 5. Sum of all tumor sizes in a single mouse were described as the tumor score.

RNA isolation

Total RNA of normal colon tissues, AOM/DSS-induced polyps, normal or tumor colonic organoids were extracted using Trizol reagent (Thermo, 15596018). Tissues and tumors were homogenized with lysing matrix D (MP bio, 116913) in 1 ml of Trizol. Organoids in Matrigel culture were mechanically disrupted and spun at 400 g and 4°C for 5 min. Pellets were re-suspended with PBS and this was repeated twice, then pellets were dissolved in Trizol. RNA cleanup was

performed using miRNeasy kit (Qiagen, 217004) with on-column DNase digestion (Qiagen, 79254) according to the manufacturer's instructions.

RNA-seq analysis

Total RNA was extracted from the AOM/DSS-induced polyps from wild type and *Lgr5*^{CreERT2}-*Dkk2*$^{fl/fl}$ mice or colon cancer organoids. RNA-seq libraries were constructed following Illumina TruSeq Stranded mRNA protocol (20020594). The RNA-seq libraries were sequenced on the Illumina HiSeq 2500 instrument platform (76 bp single-end sequencing) or Illumina Nextseq 500 (42 bp paired-end run). The sequencing reads were aligned onto Mus musculus GRCm38/mm10 reference genome using the TopHat v2.1.0 software or Kallisto v0.45.0. The mapped reads were transformed into the count matrix with default parameters using the HTSeq v0.8.0 software, then normalized using the DESeq v2 software. Differentially expressed genes (DEGs) were identified using the same software based on a negative binomial generalized linear model. Sleuth was used to analyze statistical significance of kallisto data.

Quantitative real time PCR

1-5 μg of total RNA was used for cDNA synthesis using the SMARTer cDNA synthesis kit (Clontech, 634925) following the manufacturer's protocol. Quantitative real time PCR was performed in 10 μl reactions using the iTag universal SYBR Green supermix on the CFX96 Touch™ real-time PCR detection system. PCR primers are listed in the supplementary table 1.

Organoid culture

Colonic epithelium was isolated as previously described(Andersson-Rolf et al., 2014). The isolated colonic crypts were dissolved in 50 μl of 1:1 ratio mixed Matrigel (Corning, 356231) and the IntestiCult™ organoid growth medium, STMECELL, 06005), then plated in a 24 well plate. Once Matrigel was solidified, organoids were incubated in 500 μl of the organoid growth medium. The organoid medium was replaced every other day. Recombinant mouse DKK2 protein (R&D, 2435-DKB-010) was added in a dose- and time-dependent manner. Colon tumor organoids

carrying various combinations of mutations in APC, KRAS, TP53 and SMAD4 and the tandem dimer Tomato (tdTomato) reporter gene were generated as described below. The minimal medium containing 1x B27 supplement (Thermo, 12587010), 1x Glutamax (Gibco, 35050061) and 1x Penicillin/Streptomycin (Thermo, 15140122) in advanced DMEM-F12 (Thermo, 12634010) was prepared. Those tumor organoids were plated in 1:1 ratio of Matrigel and the minimal medium mix. APC only (A), APC and TP53 double mutant (AP) organoids were cultured in the minimal medium with 50 ng/ml of EGF. APC and KRAS double mutant (AK), APC, KRAS and TP53 triple mutant (AKP) and APC, KRAS, TP53 and SMAD4 quadruple mutant organoids were cultured in the minimal medium. Culture medium was replaced every other day.

Development of colon tumor organoids

Colon crypts were isolated from

[1]: *Rosa-LSL-tdTomato* mice,

[2]: *LSL-Kras*$^{G12D/+}$ *Rosa-LSL-tdTomato* mice,

[3]: *LSL-Kras*$^{G12D/+}$*Tp53*$^{fl/fl}$*Rosa-LSL-tdTomato* mice.

Organoid lines were cultured in the WRN media with recombinant mouse EGF (50 ng/ml, Peprotech 315-09). Then, organoids were transfected with *pSECC-Apc* plasmid (containing *Cre*, *Cas9* and *sgApc*) to generate

[1] *Apc*$^{-/-}$*tdTomato*$^{+}$,

[2] *Apc*$^{-/-}$*Kras*$^{G12D/+}$*tdTomato*$^{+}$,

[3] *Apc*$^{-/-}$*Kras*$^{G12D/+}$*Tp53*$^{-/-}$*tdTomato*$^{+}$ organoids.

Apc deletion was selected by Wnt3A withdrawal, *Tp53*$^{-/-}$ was selected by Nutlin-3 addition (10 μM) and *Kras*^{G12D} was selected by EGF withdrawal. After establishment of the *Apc*$^{-/-}$ *Kras*$^{G12D/+}$*Tp53*$^{-/-}$*tdTomato*$^{+}$ organoid line, subsequent transfection with *pSECC-Smad4* plasmid (containing *Cre, Cas9* and *sgSmad4*) was performed. *Smad4* deletion was selected by addition of TGFβ (10 ng/ml) to the media to generate

[4] *Apc*$^{-/-}$*Kras*$^{G12D/+}$*Tp53*$^{-/-}$*Smad4*$^{-/-}$*tdTomato*$^{+}$ organoids.

Design and cloning gRNA/Cas9 plasmids targeting Dkk2 and Hnf4α1

sgRNAs of *Dkk2* and *Hnf4α1* were cloned into LentiCRISPRv2 or LentiCRISPRv2-blast respectively according to an established protocol (Ran et al., 2013). LentiCRISPRv2 (plasmid #52961) and LentiCRISPRv2-blast (plasmid #83480) were purchased from the Addgene (Sanjana et al., 2014). sgRNAs targeting the first exon of mouse *Dkk2* and *Hnf4α1* were designed using the Broad Institute's online sgRNA designer (https://portals.broadinstitute.org/gpp/public/analysis-tools/sgrna-design), (Doench et al., 2016). Non-targeting control gRNAs were selected from the mouse GeCKO v2 library(Sanjana et al., 2014). *Dkk2*; 5'- GTTCATGCCTGCAGATCGGT-3', *Hnf4α1*; 5'-GTAGTCGGCCATATCCATGC-3', non-targeting sgRNA; GACTCCGGGTACTAAATGTC

Lentiviral transduction

293FT cells were transfected with psPAX2, pMD2.G and LentiCRISPRv2 carrying guide RNA targeting *Dkk2* exon1 (5'-GTTCATGCCTGCAGACGGTTGG-3') using jetPEI (Polyplus, 101-10N) according to the manufacturer's protocol to generate lentivirus. Lentivirus was precipitated and concentrated by peg-IT (SBI: LV810A-1) solution. AKP organoids were digested as single or 2-3 attached cells in TrypLE solution (Thermo, 12605010) at 37 °C for 10-30 min. Approximately 100,000 isolated cells were mixed with 250 μl of the concentrated lentivirus, polybrene (8 μg/ml) and Y27632 (10 μM, Tocris, 1254) in total 750 μl of advanced DMEM-F12 and plated in a 24 well plate. Spin infection was performed at 600 g, 37 °C for 1 h, then placed in the CO_2 incubator for 6 h. The transduced cells were harvested and plated in 50 μl of Matrigel (Corning, 356231). 2-3 days after incubation in the minimal medium (B27, Glutamax and Pen/strep in advanced DMEM-F12), the transduced organoids were selected in the 10 μg/μl of Puromycin containing minimal medium for 7 days. Puromycin was refreshed every other day. Single cell sorting was performed to clone the transduced *Dkk2* knockout AKP organoids. Knockout clones have identified by sequencing the guide RNA target region.

To knockdown *Hnf4α1* in *Dkk2* knockout AKP organoids, we generated lentivirus using LentiCRISPRv2-blast carrying guide RNA targeting *Hnf4α1* exon1 (5'-

GTAGTCGGCCATATCCATGCCGG-3') as described above. After lentiviral transduction, *Hnf4α1* knockdown organoids were selected in the 10 μg/μl of Blasticidin containing minimal medium for 7 days. The culture medium was refreshed every other day.

Immunostaining and Confocal microscopy

Paraffin-embedded sections were cleared with Xylene and rehydrated with Ethanol and deionized water using standard methods. Antigen retrieval was performed using the sodium citrate buffer (10 mM sodium citrate, 0.05 % Tween20, pH 6.0) at 95°C for 30 min. Tissue sections were stained with anti-DKK2 antibody (Millipore, 06-1087) or anti-Ki67 (Thermo, 14-5698-82) antibody overnight at 4°C followed and for secondary antibody for 1 hour at room temperature. DAB staining (Vector Lab) and hematoxylin (Sigma) counter staining were performed for detection following manufacture's protocols. Images were acquired with a QImaing microscope camera. For immunofluorescence and confocal microscopy, sections were stained with anti-HNF4α1 antibody (R&D, pp-k9218), alexa488-conjugated anti-mouse IgG2a secondary antibody, anti-CTNNB1 monoclonal antibody (Invitrogen, 53-2567-42) and DAPI (Sigma, D9542). Pictures were captured using a Zeiss Axio Observer Z.1 microscope or a Zeiss LSM780 confocal laser-scanning microscope.

Tumor dissociation

Colitis-induced tumors and liver metastasized tumors were collected and dissociated in the digestion buffer containing 200 U/ml of type IV collagenase (Worthington, LS004188), 125 μg/ml of type II dispase (Sigma, D4693), 2.5 % fetal bovine serum, 1x Penicillin/Streptomycin in DMEM at 37 °C for 30-60 min with agitation. Isolated cells were centrifuged at 400 g and 4 °C for 5 min, then re-suspended in chilled PBS and filtered through the 40 μm pore size strainer.

Flow cytometry

Single cells isolated from organoids or metastatic tumors were fixed and permeabilized with the intracellular fixation and permeabilization buffer set (eBioscience, 88-8824-00) following the

manufacturer's instructions. Those cells were stained with DyLight488 conjugated anti-Lgr5 antibody (Clone: OTIA2, Origene, TA400002) or anti-phospho-Src (Ty416) antibody (Clone: 9A6, Milliporesigma, 05-677) and Brilliant violet 421 (BV421) Rat anti-mouse IgG3 antibody (Clone: R40-82, BD Horizon, 565808). Flow cytometry was performed using the Stratedigm-13.

Supplemental References

ANDERSSON-ROLF, A., FINK, J., MUSTATA, R. C. & KOO, B. K. 2014. A video protocol of retroviral infection in primary intestinal organoid culture. *J Vis Exp*, e51765.

DOENCH, J. G., FUSI, N., SULLENDER, M., HEGDE, M., VAIMBERG, E. W., DONOVAN, K. F., SMITH, I., TOTHOVA, Z., WILEN, C., ORCHARD, R., VIRGIN, H. W., LISTGARTEN, J. & ROOT, D. E. 2016. Optimized sgRNA design to maximize activity and minimize off-target effects of CRISPR-Cas9. *Nat Biotechnol,* 34**,** 184-191.

RAN, F. A., HSU, P. D., WRIGHT, J., AGARWALA, V., SCOTT, D. A. & ZHANG, F. 2013. Genome engineering using the CRISPR-Cas9 system. *Nat Protoc,* 8**,** 2281-2308.
SANJANA, N. E., SHALEM, O. & ZHANG, F. 2014. Improved vectors and genome-wide libraries for CRISPR screening. *Nat Methods,* 11**,** 783-784.